D-4

PNE-903F
FINAL REPORT

Plowshare civil, industrial and scientific uses for nuclear explosives

UNITED STATES ATOMIC ENERGY COMMISSION / PLOWSHARE PROGRAM

NEVADA TEST SITE

Reproduced From
Best Available Copy

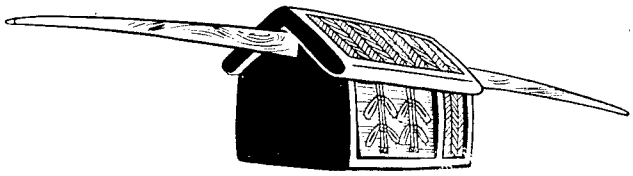

Palanquin

NEVADA
CALIFORNIA
MERCURY
LAS VEGAS

DISTRIBUTION STATEMENT A
Approved for Public Release
Distribution Unlimited

Long-Range Airblast

20000915 016

Sandia Laboratory

Albuquerque, New Mexico

ISSUED: APRIL 25, 1969

LEGAL NOTICE

This report was prepared as an account of Government sponsored work. Neither the United States, nor the Commission, nor any person acting on behalf of the Commission:

A. Makes any warranty or representation, expressed or implied, with respect to the accuracy, completeness, or usefulness of the information contained in this report, or that the use of any information, apparatus, method, or process disclosed in this report may not infringe privately owned rights; or

B. Assumes any liabilities with respect to the use of, or for damages resulting from the use of any information, apparatus, method, or process disclosed in this report.

As used in the above, "person acting on behalf of the Commission" includes any employee or contractor of the Commission, or employee of such contractor, to the extent that such employee or contractor of the Commission, or employee of such contractor prepares, disseminates, or provides access to, any information pursuant to his employment or contract with the Commission, or his employment with such contractor.

This report has been reproduced directly from the best available copy.

Printed in USA. Price $3.00. Available from the Clearinghouse for Federal Scientific and Technical Information, National Bureau of Standards, U. S. Department of Commerce, Springfield, Virginia 22151.

USAEC Division of Technical Information Extension, Oak Ridge, Tennessee

PNE-903F
NUCLEAR EXPLOSIONS-PEACEFUL
APPLICATIONS (TID-4500)

PROJECT PALANQUIN

LONG-RANGE AIRBLAST

Jack W. Reed
Sandia Laboratory
Albuquerque, New Mexico

ABSTRACT

Eight microbarograph stations measured the airborne acoustic wave from Palanquin. By use of the high-explosives calibration shots fired close in time and space to the nuclear cratering event, the airblast transmissivity for this underground burst was determined to be 0.026.

Rocket and rawinsonde upper air observations were used to calculate acoustic wave paths, times, and propagated amplitudes for comparison with observations. Some problems in correlation were encountered which could not be completely resolved, but a good general exercise in verification was allowed.

TABLE OF CONTENTS

LONG-RANGE AIRBLAST

Event Description

Project Palanquin was a nuclear experiment in hard, dry rhyolite rock executed as part of the Plowshare Program for the development of nuclear excavation. Palanquin was fired on April 14, 1965, at approximately 0514.0105 PST (1314.0105 GMT) in Area 20 of the Nevada Test Site. The resultant yield was 4.3 ± 0.4 kt. The emplacement hole, U20K, was 183 meters (600 feet) deep and extended considerably below the device placement depth at 85 meters (280 feet). Geodetic coordinates were:

Longitude	W 116°31'24.8012"
Latitude	N 37°16'49.3501"

Objectives

1. The first objective was to assure off-site safety from airblast by operation of the Blast Prediction Unit and verification by a microbarograph network.

2. A determination of the airblast transmissivity was to be made for comparison with other cratering events.

3. Calculated propagations, made from weather balloon and rocket sounding data, were to be compared with microbarograph results to give further statistics on prediction accuracy.

Background and Theory

Explosion wave propagation to long ranges in a homogeneous sea-level atmosphere may be assumed to give overpressure, ΔP, in terms of nuclear explosion (NE) yield, W, and distance or range, R, as

STANDARD $$\Delta P \text{ mb} = 357 \text{ (W kt NE)}^{0.4}\text{(R kft)}^{-1.2} \quad (1)$$

$$= 85.9 \text{ (W kt NE)}^{0.4}\text{(R km)}^{-1.2}. \quad (1a)$$

At long ranges there is little significant difference between positive and negative signal amplitudes, so peak-to-peak amplitude $P_k \approx 1.35\ \Delta P$ from close-in conditions is generally used, and

$$P_k \text{ mb} = 482 \text{ (W kt NE)}^{0.4}\text{(R kft)}^{-1.2} \quad (2)$$

$$= 116 \text{ (W kt NE)}^{0.4}\text{(R km)}^{-1.2}. \quad (2a)$$

This equation extends beyond the region where calculated hydrodynamic blast solutions are available and connects to the low pressure end of IBM Problem M[1] at R = 9000 ft (2.74 km), for W = 1 kt NE and ambient pressure P_m = 1000 mb. The exponent on R was determined by experimental HE bursts at high altitude with blast recordings of vertical, unrefracted propagations to the surface.[2] The exponent on W is a consequence of the exponent on R and the use of cube-root distance scaling laws which are generally accepted.[3]

Blast propagations from near-surface or low-altitude bursts in a real atmosphere are refracted by the stratifications of temperature and wind, which occasionally duct and focus damaging blast waves at long ranges, as happened during early Nevada nuclear tests.[4,5,6] Various atmospheric structures and types of ducting may increase the overpressures of Eq. (1) by factors of 2 to 6. As much as 15X magnification has been observed at 65 km (40 miles) from 1.2-ton (1090 kg) HE tests under jet-stream conditions.*

*Tests at Nevada Test Site, 1960, results not yet published.

On the other hand, explosive burial attenuates the source strength to a degree dependent on scaled depth of burst. The transmission factor for airblast from bursts at cratering depth has been measured on a number of events.[7-13] The transmission factor or transmissivity is defined as the ratio of overpressure from a crater shot to the overpressure expected at the same range from the same yield for a free-air burst under identical propagation conditions. It appeared to vary considerably depending also on material environment and whether an NE or HE source was used. Considerable scatter also obtained for different azimuth directions and even for different signal paths and arrival times at a given station from a single burst event. As a result, a factor of two prediction error becomes commonplace.

For the Palanquin event, a maximum credible yield of 8 kt was stated for safety analyses. Airblast transmissivity averaged 0.20 from Sedan,* but individual measurements ranged from 0.05 to 0.35.[11] Multiplication of airblast transmissivity by atmospheric magnification shows that 15 x 0.2 = 3 times the standard amplitude of Eq. (1) might occur from jet-stream ducting, or

JET STREAM $$\Delta P \text{ mb} = 2460 \ (R \text{ kft})^{-1.2} \qquad (3)$$

$$\Delta P \text{ mb} = 591 \ (R \text{ km})^{-1.2}. \qquad (3a)$$

This might cause the window breaking "threshold" of $\Delta P = 2$ mb** to be exceeded at ranges to 115 km (375,000 ft or 70 miles). Conceivably, this could hazard Indian Springs if a jet stream were in the area and winds were blowing generally from northwest to southeast.

*Sedan was 100-kt NE at 635 feet (193 m) depth of burst in desert alluvium, Nevada Test Site, July 6, 1962.

**Blast Damage Summary, Private Communication from General Adjustment Bureau, Inc., San Francisco, Calif., to Las Vegas Field Office, AEC, no date (1955), Unc.

Propagation near the surface, below about 1 km above ground, may be ducted by nighttime temperature inversions or local wind effects. In this case, a maximum of 6X atmospheric magnification could be encountered, and

INVERSION $$\Delta P \text{ mb} = 984 \ (R \text{ kft})^{-1.2} \quad (4)$$

$$\Delta P \text{ mb} = 236 \ (R \text{ km})^{-1.2}, \quad (4a)$$

which could cause window breaking to 53 km (175,000 feet or 33 miles), beyond Beatty, the nearest and most vulnerable off-site town.

Propagation ducted by the ozonosphere at about 50-km altitudes would strike near 200-km range in a band where overpressures would not exceed 0.5 mb.

For these reasons, the Blast Prediction Unit participated on Palanquin and, with some additional recording stations, gathered further information relevant to the general Plowshare airblast safety problem for cratering explosives.

A less conservative view for Palanquin, and one expected to be used in later planning, was for W = 4 kt at a deeper scaled depth, with 0.1 transmissivity from dry rock environment and 3X magnification by uncontrolled and possibly unpredictable inversion ducting. This gives only a 0.53-mb peak overpressure at Beatty. There was thus no need for extensive safety preparation; only a weather watch for jet-stream ducting was required, and measurements were made at surrounding towns for documenting possible nuisances.

In a source model for airblast from cratering explosives, originally proposed to explain Stagecoach results,[8] a relatively strong blast is carried up from the crater, gradually spreads down to the surface, and is turned into atmospheric sound ducts. This model may be used to explain the observed increase in transmission factor with distance. This transmissivity at long range appears to vary in several ways. Comparison of Danny Boy results[12] with Sedan[11] indicates that NE airblast is less from bursts in dry rock than from bursts in moist alluvium, apparently because of cavity pressure enhancement by the presence of water vapor. However, a comparison of Stagecoach[8] in

alluvium, Buckboard[9] in basalt, both 20-ton (18160 kg) HE crater events, indicates that more distant blast was transmitted from the rock environment to long ranges. This difference was not shown by close-in ground-level blast measurements. Furthermore, it appeared that large yields, with lower fundamental wave frequencies and longer positive-phase durations, may have coupled into airwaves more efficiently. All these relations, however, were taken from averages of data with large scatter. The stated conclusions cannot be made firm and confident without considerable numbers of experimental data points, so an attempt is made to get results from as many cratering tests as possible.

Propagation calculations for tropospheric ducting have been a regular part of blast prediction for atmospheric nuclear tests.[6] Only after 1958, however, have rocket measurements of ozonosphere weather conditions near 50-km altitudes been possible. There have been relatively few opportunities to make calculations and verify predictions by microbarograph blast recordings. To date, a number of minor problems have turned up from these limited experiments which may be of consequence in predicting waves from large Plowshare cratering events. There seems to be an unexpected amount of blast energy propagated into calculated "silence" zones.[11,13] A satisfactory theory and calculation for this diffraction or scattering have not been developed as yet. Also, an adequate theory for maximum magnification has not yet been obtained, although a beginning has been made for conical sonic boom wave geometry by Friedman and associates.[14] When theories for these conditions are developed, then results and data collected on cratering events will be used to help check out theoretical predictions. Under present budgetary conditions, it is easier and more economical to add parts to planned experiments than to field special blast experiments for the sole purpose of checking specific aspects of predictive theory.

The problem of air turbulence interacting with a propagating wave, in particular sonic booms, has received increased attention lately.[15] Much interest has centered around the variability of wave amplitudes in sonic booms, but this factor also seems to contribute significantly to the scatter observed in transmissivity from underground bursts.[16] Further statistical study ard data collection pertinent to this problem would be useful.

Procedure

Seven off-site microbarograph stations were established to record waves from Palanquin. An additional station was operated on-site at CP-1 because blast prediction and control people were available for the short time required. Wintertime eastward ozonosphere propagation was still expected, based on earlier rocket observations at Tonopah, White Sands, and Point Mugu.[17] Distant off-site stations were opened in the east quadrant, as shown in Figure 1. Stations were operated at Beatty and Goldfield, at relatively close range, in case significant low-level inversion propagation gave them a rumble or minor nuisance damage. Distances and bearings to each station from all shots are listed in Table I.

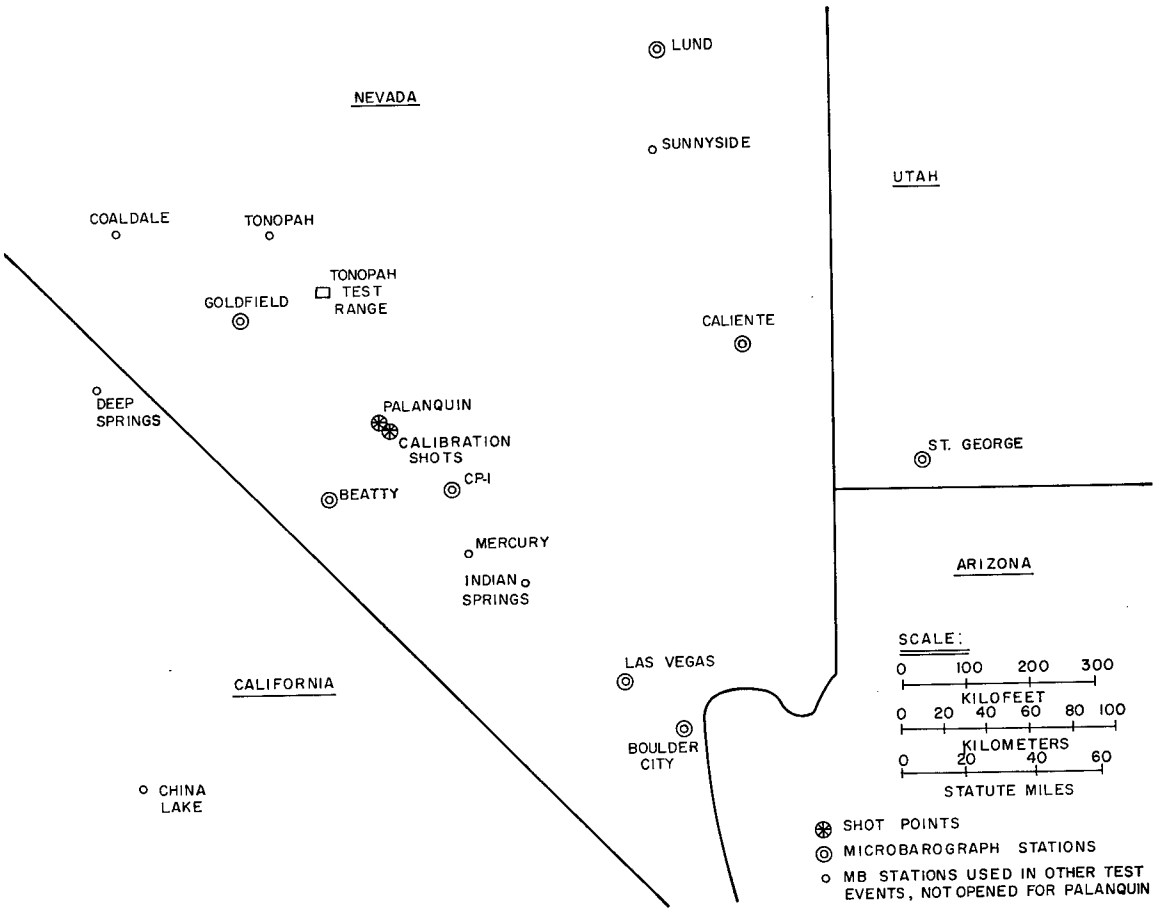

Figure 1. Palanquin shot and station locations

TABLE I

Shot and Station Locations;
Shot-to-Station Bearings, Distances

Microbarographs Stations		Shot Points			
		CAL-1 HE-20-3 37° 13' 22.8"N 116° 25' 46.3"W 6450-ft msl	Palanquin U20K 37° 16' 42.5"N 116° 31' 33.9"W 6200-ft msl	CAL-2 HE-20-2 37° 13' 30.6"N 116° 25' 38.1"W 6450-ft msl	CAL-3 HE-20-3 37° 13' 22.8"N 116° 25' 49.5"W 6450-ft msl
CP-1	36° 56' 05.3"N 116° 03' 17.8"W 4144-ft msl P = 870 mb	134.1° 151,489 ft 46.17 km	132.6° 185,794 ft 56.63 km	134.5° 151,559 ft 46.20 km	134.3° 152,362 ft 46.44 km
Las Vegas	36° 07' 57.9"N 115° 09' 30.1"W 2061-ft msl P = 941 mb	137.3° 544,624 ft 166.00 km	136.7° 578,640 ft 176.37 km	137.4° 544,732 ft 166.03 km	137.4° 545,496 ft 166.27 km
Boulder City	35° 58' 22.2"N 114° 50' 47.6"W 2461-ft msl P = 926 mb	135.0° 650,452 ft 198.26 km	134.6° 684,696 ft 208.70 km	135.1° 650,515 ft 198.28 km	135.0° 651,302 ft 198.52 km
Caliente	37° 36' 39.7"N 114° 30' 52.3"W 4380-ft msl P = 854 mb	76.3° 572,731 ft 174.57 km	78.8° 595,219 ft 181.42 km	76.3° 571,884 ft 174.31 km	76.4° 572,702 ft 174.56 km
St. George	37° 05' 37.9"N 113° 35' 27.6"W 2911-ft msl P = 911 mb	94.1° 826,744 ft 251.99 km	95.4° 855,816 ft 260.85 km	94.2° 826,103 ft 251.80 km	94.2° 826,997 ft 252.07 km
Lund	38° 52' 15.9"N 115° 00' 43.6"W 5577-ft msl P = 825 mb	34.6° 726,272 ft 221.37 km	37.3° 725,787 ft 221.22 km	34.5° 725,241 ft 221.05 km	34.6° 725,552 ft 221.15 km
Beatty	36° 56' 36.0"N 116° 42' 48.0"W 4700-ft msl P = 890 mb	218.9° 131,295 ft 40.02 km	204.0° 133,872 ft 40.80 km	218.9° 132,319 ft 40.33 km	218.6° 131,902 ft 40.20 km
Goldfield	37° 41' 48.0"N 117° 13' 42.0"W 6000-ft msl P = 818 mb	306.5° 288,788 ft 88.02 km	306.7° 254,214 ft 77.48 km	306.3° 288,842 ft 88.04 km	306.4° 287,976 ft 87.78 km

For transmissivity measurements, the atmospheric propagation must be determined for a known source. At H - 120 seconds, H + 240 seconds, and H + 420 seconds, 1090-kg HE shots were fired from 4.56-m platforms in the calibration shot area on Pahute Mesa, about 10 km from Palanquin. For comparing propagation to distances over 160 km, this separation seemed reasonable for establishing the basic propagation pattern, but there was admittedly a chance of moderate error. Time and funds for a one-time use, new HE area closer to GZ were short, so it was not established.

Waves from these HE calibration shots were recorded by all microbarograph stations, and results were scaled to the expected Palanquin yield, time, and location, but for a free-air burst. This

result divided into the observed Palanquin wave amplitudes gave the required transmission factor values.

From the weather observations and forecasts preceding the main event,* it was clear that there would be no wave focused on either Beatty or Goldfield. Moderate northwest winds near 5.5-km msl were expected to duct tropospheric waves toward Indian Springs, Las Vegas, and Boulder City. No strong focusing was indicated and the strike distance was 50 to 60 km, so any focus intensity was expected to be scattered or otherwise reduced by at least two ground reflections before arriving in Las Vegas.

Wind rockets were launched from Tonopah Test Range after Palanquin was fired. A Judi rocket motor, manufactured by Rocket Power, Inc., Phoenix, Arizona, carried a Dart payload nose to 78-km msl. This 13.6-kg system carried a 680-gm payload of copperwire chaff, each piece 5 cm long and 0.13 mm in diameter. Chaff of this size falls freely to about 60 km where air density and drag become sufficient to carry it with the wind as it falls down to around 15 km. Timed chaff-cloud tracks reported by a modified MPS-25 radar furnished wind observations through height layers. These winds were observed from altitudes of 18 km to approximately 62 km (Table II). Rawinsonde balloon observations of wind and temperature in the troposphere and low stratosphere were made by ESSA-ARFRO at Pahute Mesa from ground level to 36-km msl. Above balloon flight levels, temperatures were taken from the United States Standard Atmosphere, 1962.[18]

Weather balloon shot-time observations and rocket data were used to calculate the sound velocity versus altitude and refracting structure of the atmosphere. Ray path calculations were made for the direction of each microbarograph essentially as shown in previous reports,[6] but refined recently by Thompson.[19,20] The density of ray arrivals on the ground gives the relative airblast energy flux expected. Shot yields are then used to make actual overpressure predictions. Results were compared to recordings made by microbarographs.

*All NTS weather information is furnished by ESSA, Air Resources Field Research Office, c/o AEC Nevada Operations Office, Las Vegas, Nevada.

TABLE II

Upper Air Observations
Used for Sound Ray Calculations

	Height (kft, msl)	Height (km, msl)	Temperature (°C)	Direction (deg)	Speed (knots)	Speed (mps)	
	6.2	1.9	- 2.1	175	5	3	
	7.0	2.1	- 1.7	170	6	3	
	10	3.0	- 8.0	160	2	1	
	15	4.6	-15.4	300	6	3	
	18	5.5	-20.7	300	26	13	
	20	6.1	-24.6	280	31	16	
	25	7.6	-34.6	280	32	16	
	30	9.1	-45.2	270	48	25	
	35	10.6	-54.7	260	45	23	
	40	12.2	-49.6	250	52	27	
	50	15.2	-58.6	230	54	28	
	60	18.3	-57.9	210	18	9	
	70	21.3	-56.3	070	12	6	
	80	24.4	-53.6	110	11	6	
	90	27.4	-49.0	060	12	6	*
	100	30.4	-43.1	260	7	4	**
	110	33.5	-37.2	270	17	9	
*	120	36.6	-31.1	260	32	16	
**	130	39.6	-23.8	230	48	25	
	140	42.6	-15.4	255	54	28	
	150	45.7	- 7.0	214	30	15	
	160	48.7	- 2.5	223	30	15	
	170	51.8	- 2.5	263	45	23	
	180	54.9	- 7.3	255	60	31	
	190	57.9	-13.3	274	53	27	
	200	61.0	-19.3	270	35	18	

NOTES:

*Data above line: ESSA rawinsonde, released at Area 20, NTS, 0514 PST.

**Data below line: Winds - Sandia Corp. chaff rocket, launched at Tonopah Test Range, 1110 PST (0631 PST track plot in error)
Temperatures - USSA-62 Standard Atmosphere.[18]

The microbarograph equipment was the same as has been used for several years in distant airblast recording.[21] Differential pressure-wave sensors were twisted bourdon tubes which turned an armature with respect to an E-core. Varying reluctance in the E-core modulated a carrier wave transmitted by a coaxial line into the appropriate signal amplifiers for recording. Sensor heads were manufactured by Wiancko Corporation, Pasadena, California, as specified and evaluated by Sandia Corporation.[22] Amplifier and timer systems in current use were designed at Sandia and built by the Electronic Engineering Company, Santa Ana, California. Brush Electronics Company pen-type recorders were used at a paper speed of 2.5 cm/sec, with 1-second time

marks provided by an event-marking pen. Zero-time signals for both calibration and Palanquin shots were transmitted on NTS Net 12 radio and recorded on each pressure trace. The combined instrument and recorder response time for pressure signals was such that 95 percent of pen deflection from a square-wave pressure pulse would be recorded in about 15 milliseconds. Thus, there was very little amplitude damping for signals having frequencies lower than 10 Hz.

A major recent refinement is that a simple snow-fence wind noise attenuator[23] was placed on a 3-m radius circle around the microbarograph sensor. Tests have shown that ambient wind noise amplitudes can be reduced by a factor of 6 without significantly reducing the shock-wave amplitudes from charges as small as 116 kg.

Results

There was no audible signal from Palanquin reported at any off-site microbarograph station or town. The maximum amplitude recorded off-site was 20.3 μb at Lund, while the calibration shots gave Lund as much as 68.3 μb, barely in the audible range. At the closest station, Beatty, calibration shots gave only about 5 μb, while Palanquin produced 8.8 μb. Propagation was weak in the Beatty direction, only 0.045 of standard for 1090 kg of HE in a homogeneous atmosphere. There was no effective ducting inversion, and the waves were refracted upward away from ground. On the other hand, observations with jet-stream ducting and focusing have shown propagations over 300 times as strong as were recorded at Beatty. It is conceivable, but extremely unlikely, that the Palanquin airblast source strength could have caused pressure amplitudes (peak-to-peak) in excess of the window-breaking level (4 mb) at Beatty had the winds been unfavorable.

A complete tabulation of microbarograph results from calibration shots is shown in Table III. Each significant signal from the calibration shots recorded at each station is described, along with arrival time in seconds after the shot, peak-to-peak pressure amplitude in microbars, average or group velocity in meters per second and feet per second, the atmospheric magnification or focus factors, and

TABLE III

Calibration Shot Microbarograph Data Summary

Station	Signal	Calibration Shot 1, H - 2 Minutes 0512 PST					Calibration Shot 2, H + 4 Minutes 0518 PST					Calibration Shot 3, H + 7 Minutes 0521 PST					Signal Duct
		Travel Time (sec)	Group Vel. ft/sec	Group Vel. mps	Pressure Amplitude (μb)	Focus Factor (F)	Travel Time (sec)	Group Vel. ft/sec	Group Vel. mps	Pressure Amplitude (μb)	Focus Factor (F)	Travel Time (sec)	Group Vel. ft/sec	Group Vel. mps	Pressure Amplitude (μb)	Focus Factor (F)	
CP-1		144.31	1050	320	66.1	0.555	142.90	1060	323	64.4	0.540	143.40	1061	323	91.0	0.764	T
Las Vegas	a	(1)					511.40	1062	324	4.6 (3)	0.17	~511	~1068	~325	(2)		T
	b	(1)					576.34	943	287	5.3	0.195	579.45	943	287	8.1 (3)	0.298	Z
Boulder City	a	606.5	1071	326	9.6	0.442	604.0	1079	329	10.8	0.497	~604 (1)	~1080	~329			T
	b	682.1	955	291	6.0	0.276	677.9	961	293	16.2	0.746	677.5	963	293	22.2	1.022	Z
	c	692.7	940	286	6.0	0.276	692.2	940	286	9.0	0.415	692.9	942	287	6.0	0.276	Z
Caliente	a	627.90	950	289	43.6	1.894	626.4	950	289	23.3	1.012	628.0	950	289	33.3	1.447	Z
	b	639.01	934	284	36.9	1.603	637.4	934	284	37.5	1.629	638.9	935	285	20.3	0.882	Z
St. George	a	850.1	971	296	8.02	0.497	845.9	977	297	3.30	0.204	847.0	976	297	4.63	0.287	Z
	b	854.1	969	295	9.50	0.589	849.9	974	276	10.33	0.640	850.8	971	296	8.88	0.550	Z
	c	903.3	916	279	15.1	0.935	901.9	916	279	10.14	0.628	902.9	916	279	9.70	0.601	Z
	d	912.0	907	276	44.4	2.750	910.8	907	276	28.8	1.784	911.8	907	276	16.1	0.997	Z
Lund	a	749.78	970	295	60.0	3.390	747.80	970	295	68.3	3.860	749.91	969	295	63.5	3.590	Z
	b	754.58	963	293	24.9	1.408	752.89	964	293	34.1	1.927	755.09	961	293	52.1	2.945	Z
Beatty		(4)			4.8	0.034	123.9	1072	326	6.4	0.045	124.5	1065	324	5.6	0.039	T
Goldfield		(5)					(5)					~264	~1090	332	(3)	<0.185 (6)	T

Remarks:
(1) No record, equipment troubles.
(2) Pen adjustment obscured record.
(3) Low signal-to-noise ratio.
(4) Timing troubles, uncertain.
(5) Communication trouble, not recording.
(6) Wind noise 10 μb, occasional peaks to 25 μb.

appropriate remarks. Group velocity was obtained by dividing shot-to-station distances from Table I by travel time. Signal paths are identified by their velocity, i.e., arrivals faster than about 1050 ft/sec (320 mps) were ducted by troposphere winds, while slower arrivals were ducted by the ozonosphere. No ionosphere signals, which are reflected by high-temperature layers above about 100-km altitudes, were found on any of the records. They have not been found by this network for these source strengths in the past, although they were frequently observed from full-scale atmospheric nuclear tests.

Atmospheric focus factors result from dividing observed amplitudes by the standard amplitudes determined by Eq. (1). For 1090 kg of TNT burst at 4.56 m above ground, or 1.12 ft/(1b HE)$^{1/3}$, height of burst enhances the blast[24] so that it equals the strength from 1930 kg of HE[25] or 4.25 x 10^{-3} kt of NE free airburst. Since peak-to-peak amplitude, P_k, is about 1.35 ΔP[1], the standard amplitude for calibration shots at sea level is obtained by substitution in Eq. (1):

$$P_k \text{ mb} = 54.4 \ (R \text{ kft})^{-1.2} \tag{5}$$

$$= 13.1 \ (R \text{ km})^{-1.2}. \tag{5a}$$

This is corrected for standard atmospheric pressure, P_s, at the recording station by using

$$P_k = 13.1 \left(P_s/P_m\right)^{0.6} (R \text{ km})^{-1.2}. \tag{6}$$

Results from Palanquin are shown in Table IV, again including travel time, group velocity, and amplitude. Free-air burst standard amplitude, for W = 4.3-kt NE and including the appropriate correction for standard atmosphere[18] station pressure, which is shown in Table I, is given by

$$P_k \text{ mb} = 3.28 \left(P_s \text{ mb}\right)^{0.6} (R \text{ km})^{-1.2}. \tag{7}$$

TABLE IV

Palanquin Microbarograph Data Summary

Station	Signal	Travel Time (sec)	Signal Duct	Group Velocity (ft/sec)	Group Velocity (mps)	Pressure Amplitude (μb)	Free Airburst Std Amplitude (μb)	Free Airburst Amplitude Scaled from Calibration Shots CAL-1	CAL-2	CAL-3	Transmission Factors CAL-1	CAL-2	CAL-3
CP-1		174.24	T	1066	324	33.5	1500	1110	1081	1379	0.0302	0.0310	0.0243
Las Vegas	a	538.4	T	1074	327	8.1 (1)	402	-	74	-	-	0.0690	-
	b	606.5	Z	952	290	4.8		-	135	181	-	0.0356	0.0265
Boulder City	a	635.5	T	1077	328	9.6	331	196	216	-	0.0489	0.0444	-
	b	710.7	Z	962	293	7.8		137	283	356	0.0569	0.0276	0.0219
	c	722.9	Z	948	289	6.0		137	186	137	0.0438	0.0323	0.0438
Caliente	a	644.86	Z	959	292	13.2 (3)	366	605	384	498	0.0218	0.0344	0.0265
	b	655.84	Z	942	287	9.15 (3)		535	535	349	0.0171	0.0171	0.0262
St. George	a	871.6	Z	982	299	1.78	247	156	116	137	0.0114	0.0153	0.0130
	b	875.6	Z	977	297	3.80		183	262	236	0.0208	0.0145	0.0161
	c	928.7	Z	923	281	4.75		253	261	253	0.0188	0.0182	0.0188
	d	937.5	Z	914	278	17.7		548	198	131	0.0323	0.0894	0.1349
Lund	a	746.92	Z	973	296	20.3	282	733	809	758	0.0277	0.0251	0.0268
	b	752.74	Z	965	294	9.2		336	484	661	0.0274	0.0190	0.0139
Beatty		125.1	T	1068	325	8.8	1974	273	328	307	0.0322	0.0268	0.0286
Goldfield		(2)					1001	-	-	-	-	-	-

REMARKS: (1) Pen adjustment may have affected signal.
(2) Communication trouble, not recording.
(3) Electrical noise amplitude 8 μb.

Each recorded calibration shot signal in Table III was used to make an amplitude extrapolation for Palanquin yield, but free-air burst. The effects of nonstandard observed amplitudes on the yield-scaling exponent[26] were included in obtaining values shown in Table IV. These amplitudes, divided into observed wave amplitudes, give the tabulated transmission factors.

Signals recorded by the CP-1 microbarograph are reproduced in Figure 2. Since the Brush recorder pen is about 7.5 cm long, it sweeps an arc in attempting a vertical line, as shown. Paper feeds from left to right through the recorder, so time increases to the left. Labeled times are in seconds after the Palanquin zero tone signal. Vertical scale varies slightly from shot to shot. It is checked by frequent calibration signals, and the calibration mark closest to each received signal is used to determine the local amplitude scale.

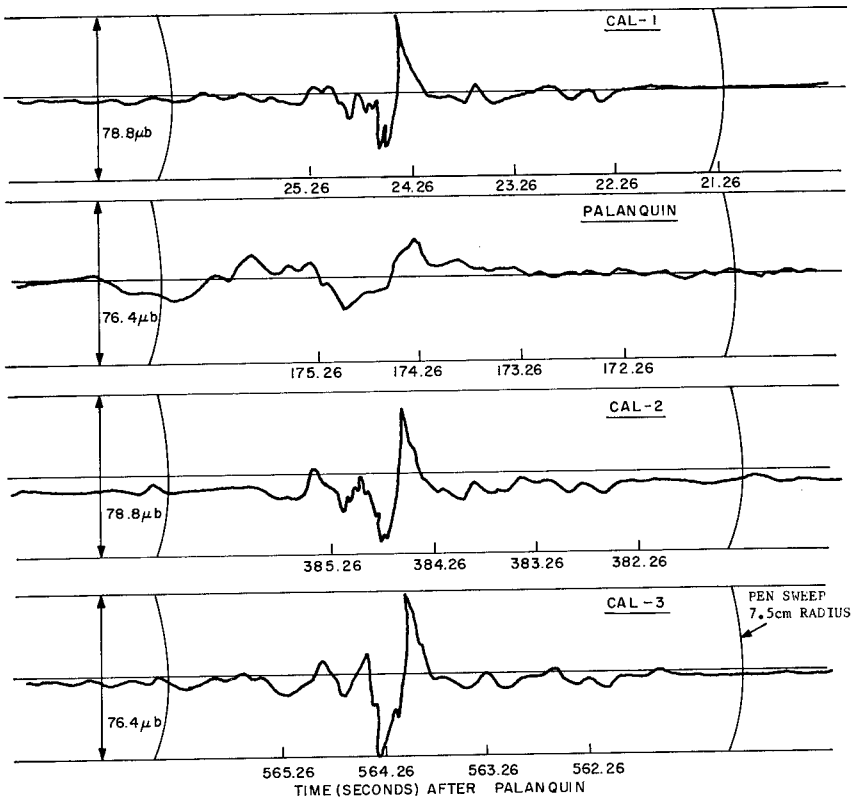

Figure 2. Microbarograph recordings at CP-1

Off-site signals were generally of low amplitude. The most interesting and clear recording was made at St. George, Utah (Figures 3 and 4). Signals "a" and "b" from Tables III and IV arrived traveling at about 299 mps (Figure 3). The later arrivals, signals "c" and "d", traveling near 280 mps, are shown in Figure 4.

In general, Palanquin signals had frequency contents which were similar to but of lower frequency than the calibration shots. Had Palanquin been airburst, however, the overpressure duration at CP-1 would have been about 0.6 second[1] and the negative phase duration about 1.6 seconds, so the total duration of the main wave would have been about double that recorded in Figure 2. At long range, positive and negative phases are longer and tend to be more nearly equal, and the St. George cycle duration would likely have been nearly 5 seconds[27] rather than the 2 seconds indicated by Figures 3 and 4.

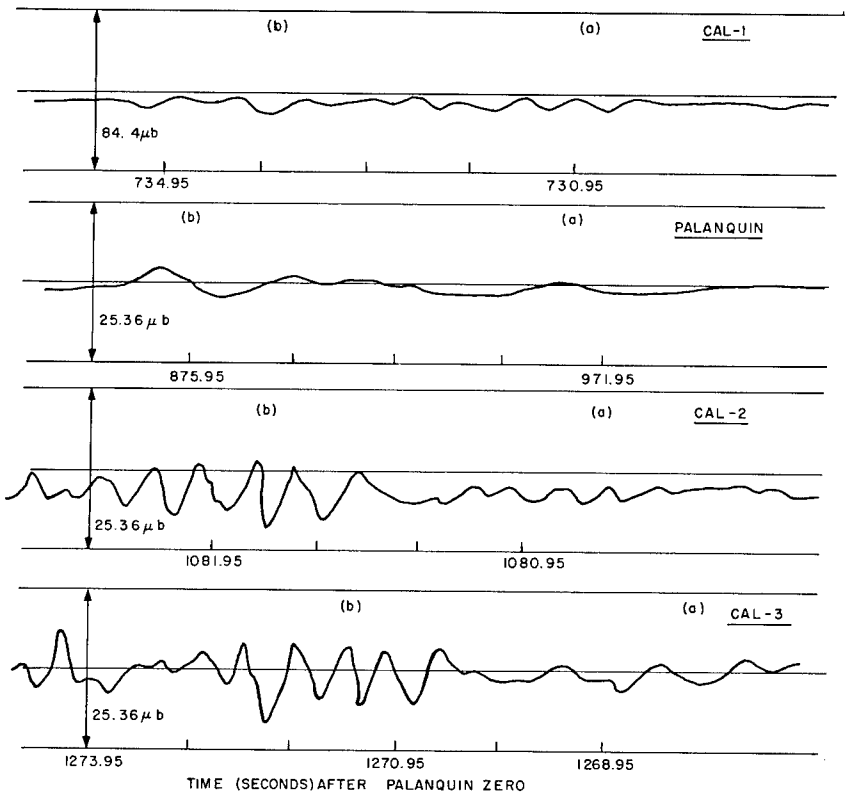

Figure 3. Microbarograph records of early signals at St. George, Utah

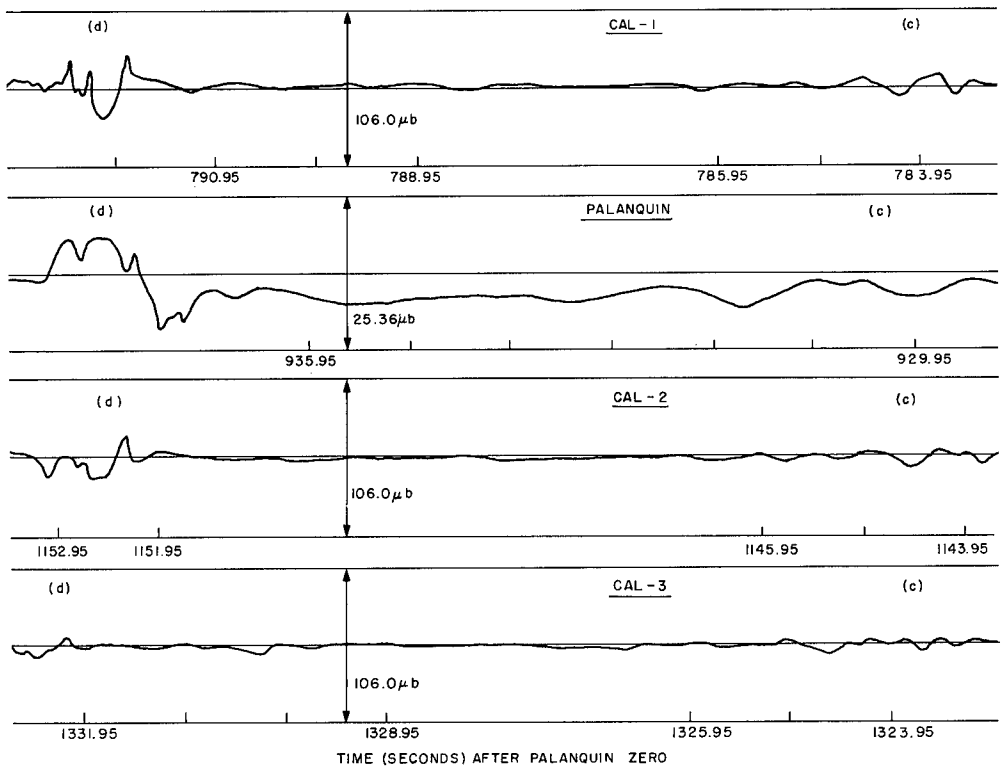

Figure 4. Microbarograph records of late signals at St. George, Utah

Palanquin transmissivities are compared with results from other cratering tests in Figure 5. The predominant feature is the much lower transmission factor it gave. The low value apparently cannot be attributed to yield uncertainty or to the rock environment. Neptune data probably are not valid for comparison because proper atmospheric calibration was not made on that event (WT-9006), but Danny Boy, Dugout, and Buckboard results, even in their extremes, do not allow transmissivities lower than 0.04. The conclusion may be made that airblast amplitudes were reduced by a factor of 3 or 4 by the shaft which extended over 300 feet below the shot point.

On the other hand, because of the nature of this explosion event--it did not blow, but it spewed--most other Palanquin effects were likewise anomalous. For useful predictions of Plowshare activities, it must therefore be ignored.

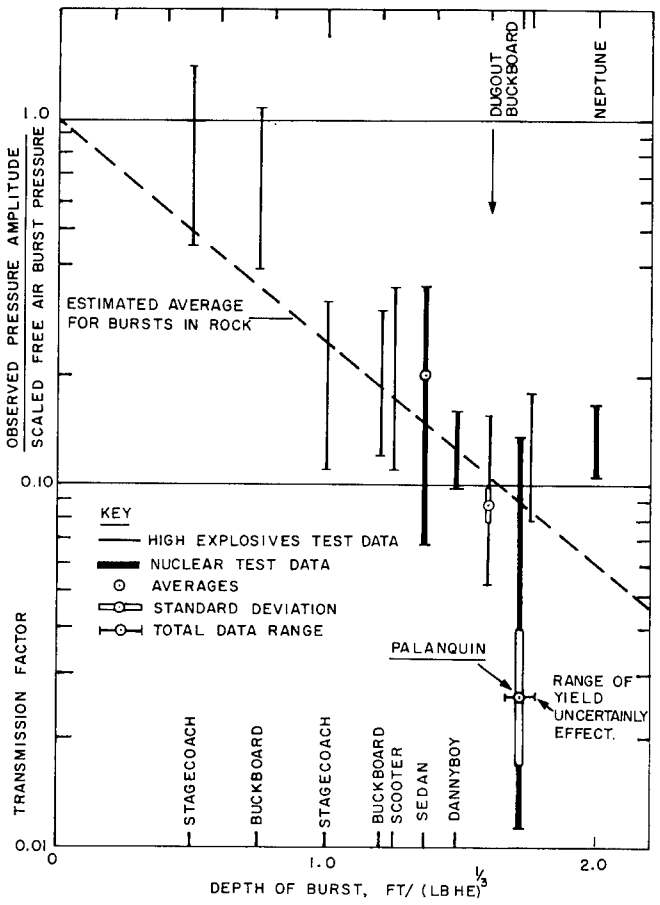

Figure 5. Airblast transmissivity versus scaled burst depths for cratering explosions

An exercise with transmissivity scaling for a measured pressure shows that a reduced assumed yield at fixed depth would increase the scaled depth of burst and also increase the transmissivity. On Figure 5, the path of the $\overline{T}$ point would move to intersect the dashed diagonal line with an assumed yield of 1.7 kt, DOB = 2.34 ft/(lb HE)$^{1/3}$, and $\overline{T}$ = 0.038. This apparent yield is in good agreement with similar interpretations of close-in measurements by Vortman,[28] which suggests a 2-kt apparent yield.

Signal variability between calibration shots, supposedly from propagations under identical conditions and only minutes apart, was particularly noticeable at St. George. This was studied and reported

separately[16] so details are not repeated here. It was established that in the time scale of minutes between calibration shots, signals would be repeated only within a factor of $(1.60)^{\pm 1}$ for the standard deviation range in a logarithmic normal distribution. Furthermore, a similar analysis of Dugout data also reached this conclusion, giving a factor of $(1.43)^{\pm 1}$ for an ensemble of 2, 3, and 5-minute shot separations. Palanquin separations were 3, 6, and 9 minutes.

Scatter of transmissivities from Palanquin agreed very well with this scatter of repeatability, as shown by the logarithmic distribution in Figure 6. Neglecting the three large reported values where $T \geq 0.0894$, the scatter factor was 1.57. One of the largest values was obtained from the tropospheric signal at Las Vegas and may well have been erroneous because the operator was adjusting the recorder pen zero-value near signal arrival time, so the apparent amplitude reading may well have included some mechanical pen shifting.

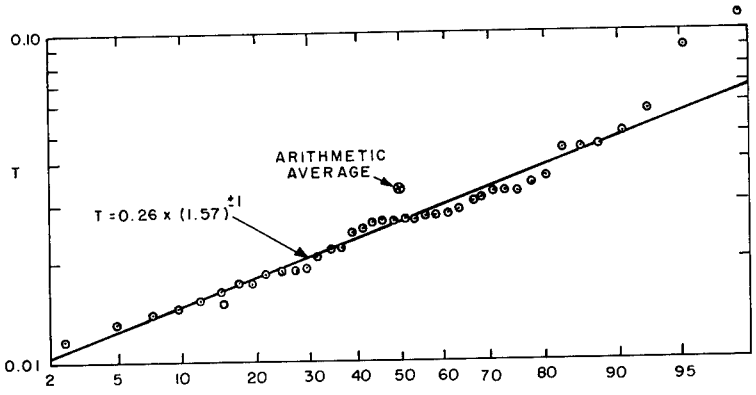

Figure 6. Distribution of transmissivity values

The other two large values resulted from the "d" signal at St. George (Figure 4). For CAL-1, three distinct pulses are shown, and all decay considerably by CAL-2 and CAL-3. From Palanquin, with its longer wavelength, these three waves apparently caused constructive interference and a resultant large amplitude. This effect cannot be disregarded in predicting for large yield, low frequency signals, for it has happened before in full-scale atmospheric nuclear testing, but these results may rationally be discounted in discussing random signal variability.

A mean transmissivity for Palanquin thus appeared to be T = 0.026, rather than an arithmetic average of all data where T = 0.033. The logarithmic standard deviation was 0.451, so that the $\pm 1\sigma$ range extended from 0.64 to 1.57 T, or T = 0.017 to T = 0.041. Neither the mean nor standard deviation varied appreciably between results of separate calibration shots, i.e., various small time separations of 2, 3, and 5 minutes caused no noticeable time-dependent effect.

The arithmetic average transmissivity from troposphere signals is 0.042 which is larger than the ozonosphere average of 0.030, but this difference was mostly caused by the probably erroneous Las Vegas value. Furthermore, it seems that troposphere ducting would have affected the rays emitted at a lower elevation angle which, according to our cratering airblast source model, should have shown lower transmissivity. With these limited statistics, therefore, no significance can be attached to this anomalous result.

It would have been interesting to see the effects of the St. George multicycle "b" signal in Figure 3 for a Palanquin blast fired about 3 minutes after Palanquin was actually fired. But then the "d" signal constructive interference would not have been so evident. The point to be made is that nonscalable constructive interference of lower frequency waves will occur quite often, so the few extremely high transmissivities which were reported do not follow the normal statistical distribution caused by atmospheric turbulent transmission variability alone.

Weather data for propagation calculations are given in Table II which lists air temperatures and wind vectors versus altitudes above sea level (msl). The ESSA rawinsonde balloon rose to 35.8 km (117,717 ft), an exceptional ascension.

Immediately after the Palanquin event was confirmed, a chaff rocket round was fired at Tonopah Test Range at 0631 PST. At 1110 PST, about 6 hours after Palanquin, a second TTR rocket was launched to check wind variations. Both flights are reported in Table II.

Rocket temperature observations were not made, so the temperature and speed of sound determinations above balloon heights were made

using a standard atmosphere.[18] Error from this temperature assumption probably does not exceed ±15°C. This would give only a ±9 mps sound speed error which is smaller than chaff wind measurement error[29] and probably not significant in its effect on ray calculations.

Ray calculations were made from the weather data for the direction bearings to each microbarograph station. Observed pressure amplitudes from calibration shots were compared with calculated ray patterns and predicted overpressures. Observed and calculated signal arrival times were compared to see if the correct ducting level had been shown in the calculation.

There was a great difference in wind speeds reported by the two rocket observations. The early flight gave high speeds, while the later flight gave speeds only 30 to 40 percent as large plus some direction changes. The differences seemed much too great for atmospheric variation in a 5-hour interval. Rawinsonde data by ESSA showed light winds at altitudes where the two measurements overlapped. However, an observation on April 9 showed high wind speeds, so at first the high-speed 0631 PST data were accepted, and the difference was attributed to a mistake in setting the radar plotting-board scale-switch during the second observation.

When reports from other stations were received,[17] however, it appeared that lower speeds were generally found during the entire month and at all stations such as Point Mugu, California; White Sands Missile Range, New Mexico; and Cape Kennedy, Florida. After ray-tracing calculations were made for both sets of wind data for verification by microbarograph reports, a number of difficulties were found which could not be explained by either wind report without significant adjustment. This is discussed in detail, station-by-station, in succeeding sections, but the most acceptable conclusion, however weak, seems to be that the light wind data should be used.

CP-1

Ray calculations showed ducting by winds in the 4.9 to 5.5-km altitude layer, with sound returned to ground level at about 5 km beyond CP-1 (Figure 7). At CP-1, the lowest part of the calculated

wave passed about 1 km overhead. Nevertheless, because of either atmospheric scattering or nonrepresentativeness in the weather observation, there was a maximum measured amplitude from calibration shots which was about 32 percent as large as the calculated wave of 341 μb which passed overhead.

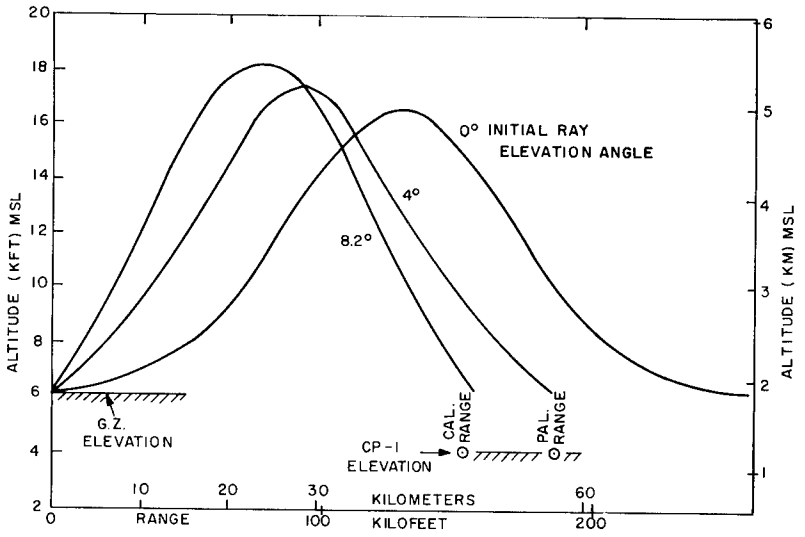

Figure 7. Ray paths calculated toward CP-1

At the 57 km range of CP-1 from Palanquin and with a slightly smaller calculated focus factor, a calibration shot wave would have hit the station with 210 μb. This would have yielded a transmission factor of only 0.013 for Palanquin. Instead of accepting this extrapolation to so low a transmissivity, a more likely conclusion is that the actual ducting and focusing were not so sharp. Then, the lower calculated amplitudes were spread over a wider band to include CP-1, and this resulted in higher calculated transmission factors. The actual values calculated for CP-1 (Table IV) are in reasonable agreement with off-site data, although they may be a bit high. At any rate, the calculated ray pattern indicates, if anything, that CP-1 transmissivities may well have been measured to give values that were too high.

As shown by Figure 8, there was quite good agreement between calculated and observed arrival times. Observed group velocities were high by less than 1 meter per second. Observed arrival times were early by less than half a second. From these results, it appears that CP-1 signals were definitely ducted by a layer at an altitude of about 5 km. Propagation in the 2-km altitude layer would have traveled at about 331 mps and arrived 2 seconds earlier.

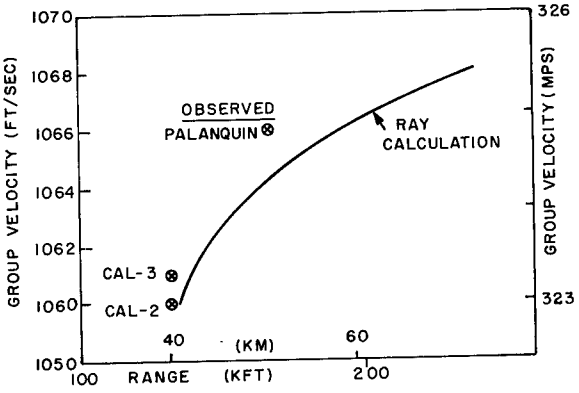

Figure 8. Calculated and observed group velocities at CP-1

Beatty

There was no troposphere ducting calculated to strike the ground in the direction of Beatty. Rays were bent upward away from the ground (Figure 9) and passed 2 km above the station. Near horizontal propagations are also diverged so that at 2 to 6 km above Beatty, the blast amplitude was only about 0.48 of standard. The 6.4-μb scattered wave recording is less than 10 percent of the probable source amplitude and thus shows that less than 1 percent of the acoustic energy flux was being scattered to ground level. Arrival time calculation also agreed well with observed arrival, with only about 1 meter per second discrepancy.

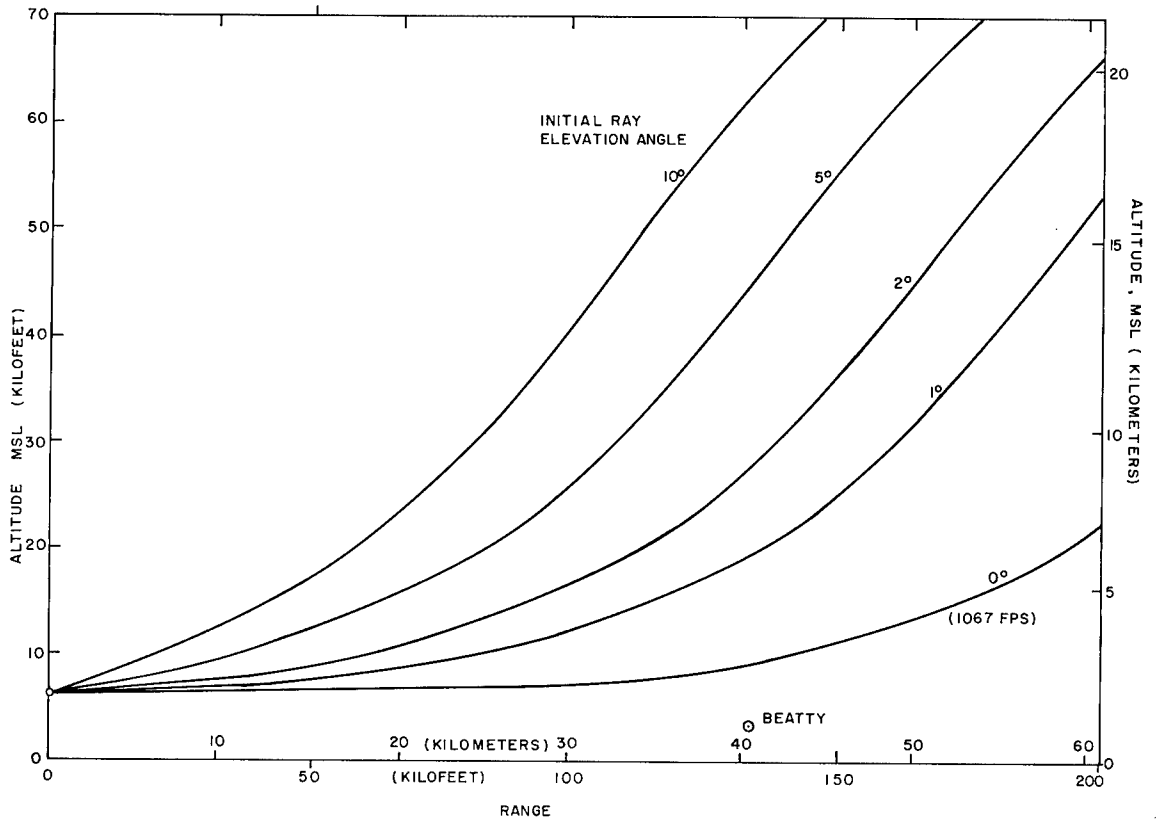

Figure 9. Ray paths toward Beatty

Goldfield

Although no signal was observed at Goldfield in the 10-μb background wind noise, rays were calculated (Figure 10) to explain the lack of signal. There was a calculated ducting in the surface layer 240-m deep, but this wave apparently was blocked by many hills along the route. Near this azimuth, several hills reach near or over 2.5-km msl; the GZ was at 1.9-km msl.

Clearly, no ozonosphere signal was expected because the wave was shown to pass Goldfield at an altitude of over 40 km. A much larger source wave, from a nuclear airburst, for example, would have given a weak, scattered signal arrival near 307 seconds. It would have come from the wave passing near 16-km altitude and 40-km range. The diffracted wave amplitude for the calibration shot yield would have been

no more than 5 percent of standard propagation, or 3 μb, and much below the 10-μb wind noise level.

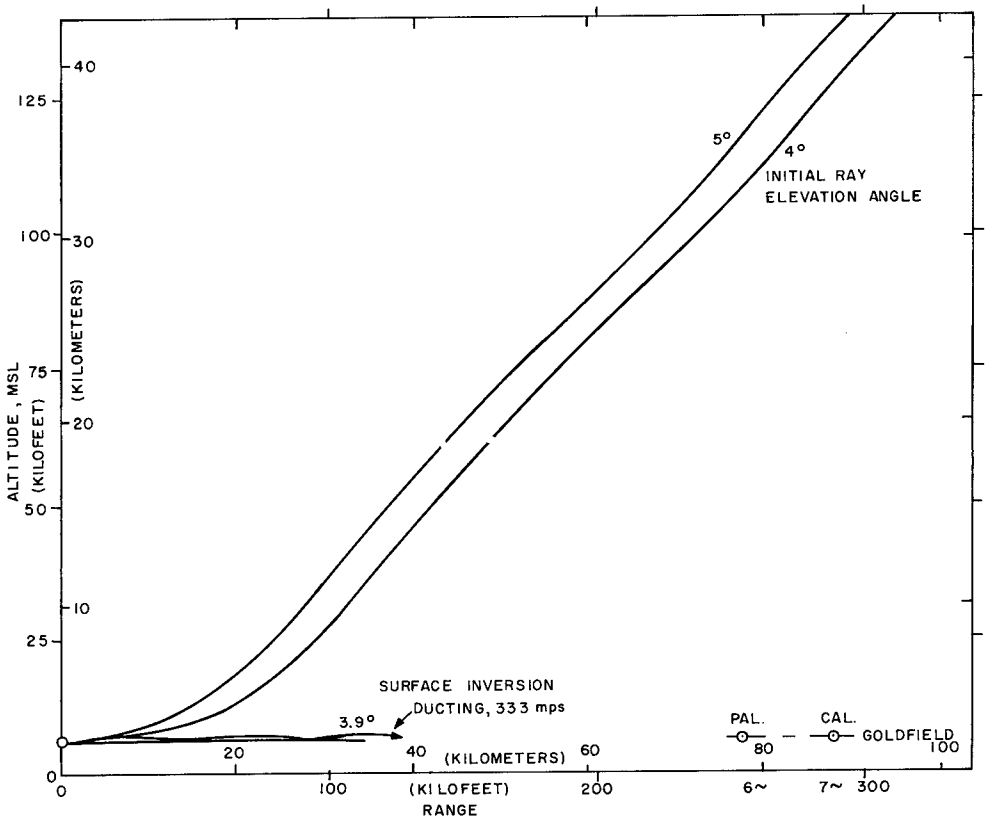

Figure 10. Ray paths toward Goldfield

Las Vegas and Boulder City, Nevada

Calculated ray paths in the general southeast direction are shown in Figure 11. Solid line curves were made using light wind data from the 1110 PST rocket report; high wind speeds from the 0631 PST rocket gave the dashed line curves on this and subsequent ray-trace figures. Separate calculations were made for CP-1, Las Vegas, and Boulder City at bearings of 134, 137, and 135 degrees, respectively, but they differ only slightly. Inner boundaries to the sound ring ducted near an altitude of 5.5 km varied by only 1.1 km; this is of little significance at 50 km. Calculated and observed group velocities are shown in Figure 12, and pressure amplitudes are shown in Figure 13.

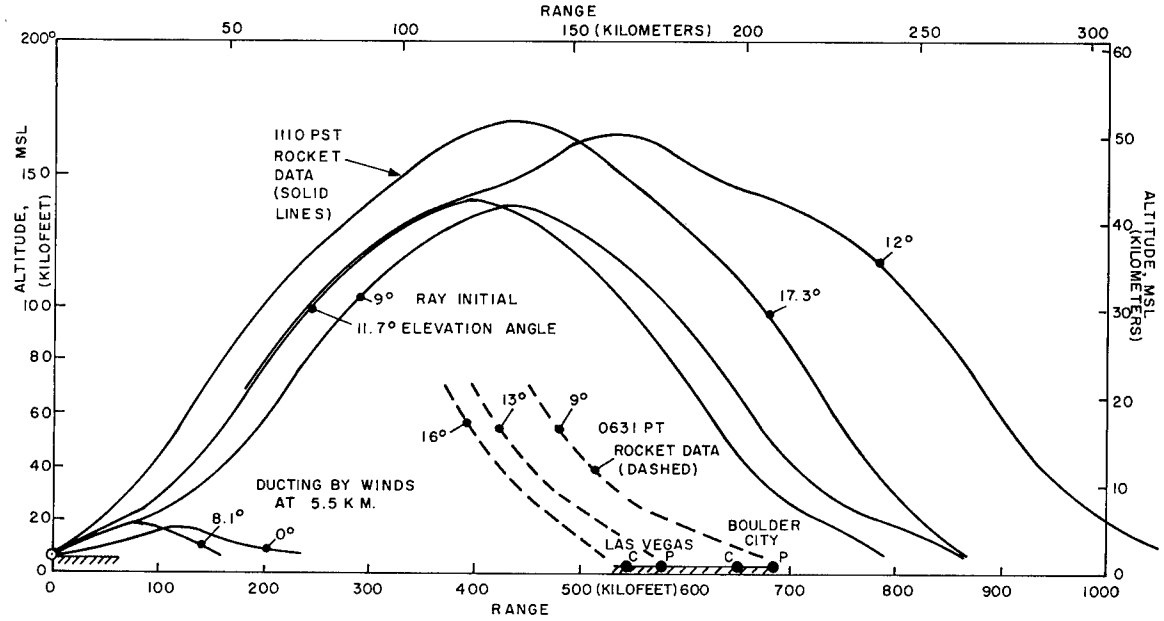

Figure 11. Ray paths toward southeast direction

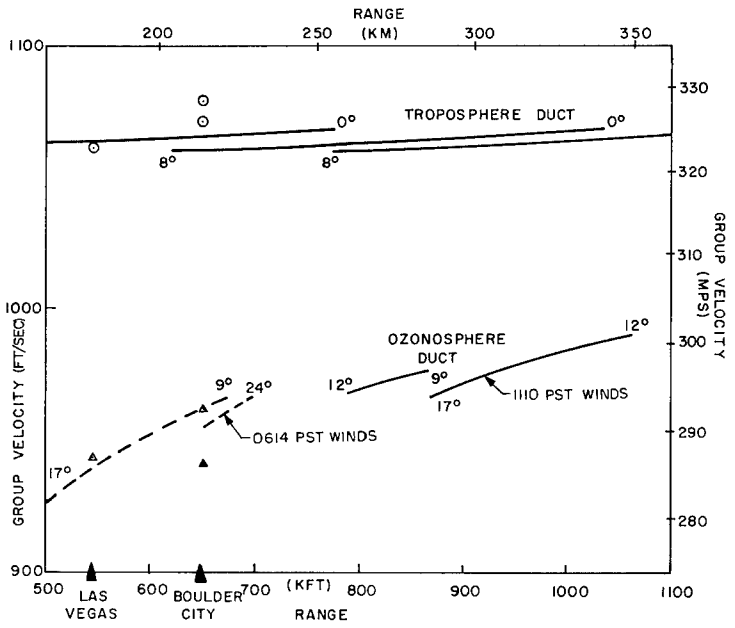

Figure 12. Calculated and observed group velocities, southeast direction

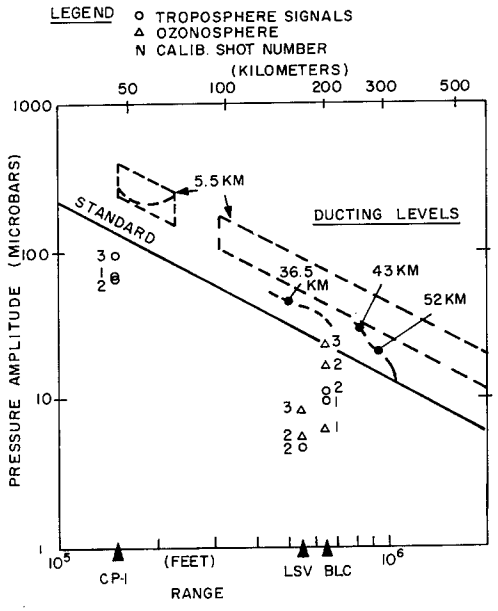

Figure 13.

Calculated and observed pressure amplitudes, southeast direction

Troposphere ducting was shown to give signals at Las Vegas and Boulder City which had been reflected by ground two to six times. The group velocity was calculated to fall between 323 and 325 mps. Reported signal arrivals agree well with this calculation, as shown in the upper part of Figure 12. The amplitude at Las Vegas is low, however, for the one troposphere arrival time when the equipment was operating (Figure 13). Calculated troposphere amplitudes are about double the standard propagation amplitude, as shown by the dashed belt in Figure 13, while at CP-1 and Boulder City the observed signal focus factors were nearer 0.5. At Las Vegas, only one-sixth standard amplitude was recorded. Although there are 3 to 5 μb of noise on the recording, nothing occurred comparable to the 13-μb value obtained by interpolating between CP-1 and Boulder City. The operator had equipment trouble earlier and may have not correctly switched the set range. Such an assumption could be used to correct the low amplitudes from both troposphere and ozonosphere duct signals.

Ozonosphere ducting from the 1110 PST rocket data show that all rays land more than 40 km beyond Boulder City (Figure 11). The high-speed wind data give a strong wave prediction for both Las Vegas and Boulder City, with larger amplitudes at Las Vegas (Figure 13). If an operator error in switching at Las Vegas is assumed (an adjacent

switch point gives a scale factor larger by a factor of 3), the average Las Vegas ozonosphere signal amplitude is larger than at Boulder City and is in agreement with the trend of the dashed curve (0614 PST). Alternatively, light wind data would not predict such strong signals at Boulder City from scattering into the silence zone but might predict that Las Vegas amplitudes would be the smaller of the pair.

Arrival times and group velocities for both stations agree well with calculations from the 0614 PST, high-speed data. If wind speeds at 1110 PST at the 42.6-km level were increased by 20 mps, however, a 17-degree ray would have been calculated to land near Boulder City at about the correct group velocity. The amplitude would have been calculated to be at least twice too large, however, so possibly a compromise 10-mps correction and some scattering gives the best overall conclusion.

St. George, Utah

Ray paths calculated from the 1110 PST rocket are shown in Figure 14. Group velocities for each wind set are shown in Figure 15, and pressure amplitudes are shown in Figure 16. The main sound ring strikes St. George in the light wind calculation. Verification of calibration shot amplitudes can be made almost equally well from either wind assumption. The high wind case does not give amplitudes as large as were observed but it does give two distinct signals, as observed, and it shows the latest arrival as having the largest amplitude. Use of the light wind data would allow an explanation of the second signal by assuming a small increase in winds at 50 to 55-km altitudes, but arrivals would be relatively weak and this is the reverse of the observed condition.

Troposphere signal arrival velocities are about right for the ducting which was calculated from near 6-km msl. Observed amplitudes are much more attenuated than expected from three ground reflections. Horizontal variations in the strong winds at 6 km probably led to considerable duct leakage and amplitude reduction from 35 μb to the observed 11 μb and less.

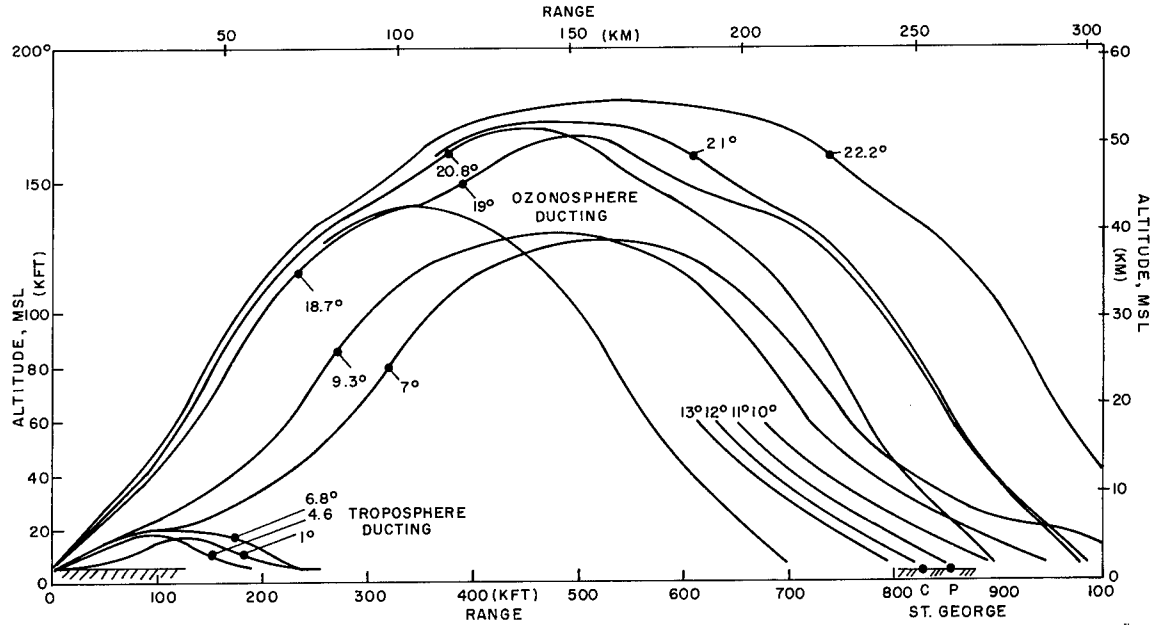

Figure 14. Ray paths toward east, St. George, 1110 PST rocket data

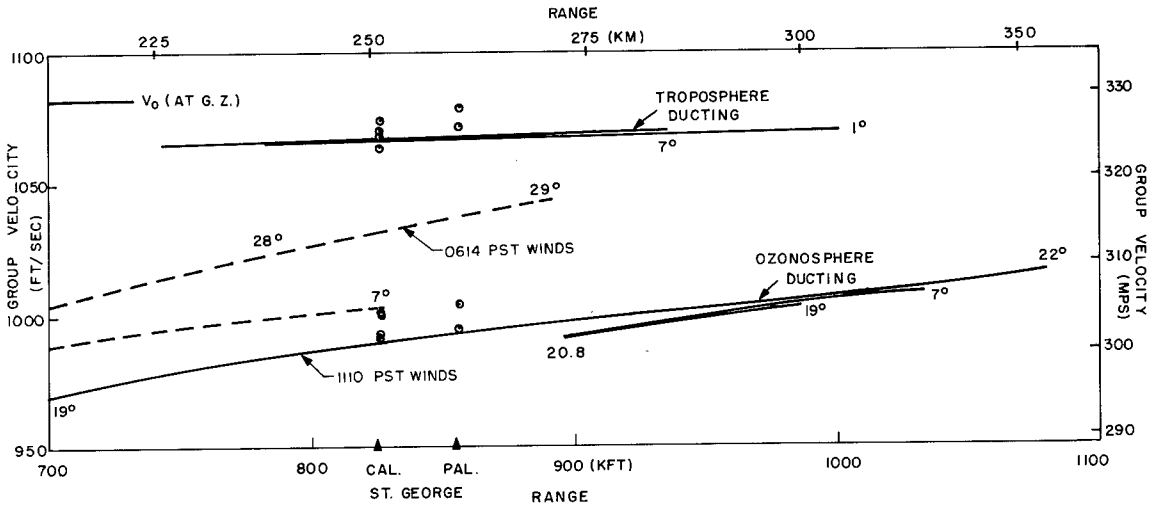

Figure 15. Calculated and observed group velocities, east direction, St. George

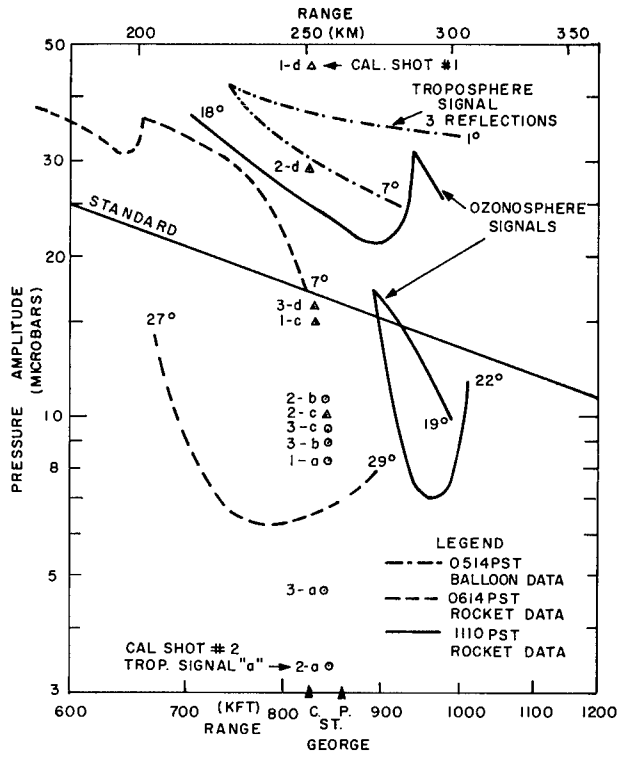

Figure 16. Calculated and observed pressure amplitudes, east direction, St. George

Caliente, Nevada

Ray calculations for light winds showed that the ozonosphere sound ring began near 216 km, at least 30 km beyond the station. Observed focus factors in Table III ranged from 0.9 to 1.9, however. High wind calculations indicated a sound ring landing on Caliente from winds at 33.5-km msl and another band arriving slightly later and with a bit less amplitude from 42.6-km msl winds. Amplitude variability in Table III shows that on the first and last shots the first wave had larger amplitudes, while for the second shot the largest amplitude was recorded from the last wave arrival.

As shown in Figure 17, group velocity calculations do not agree with observations. Calculated arrivals for the high wind assumption were too fast, while low winds gave no arrivals at such short range.

Again, as for the southeast bearings, a moderate wind speed increase could be hypothesized to contract the sound ring into Caliente range. Then observed group velocities would also come into good agreement with calculations.

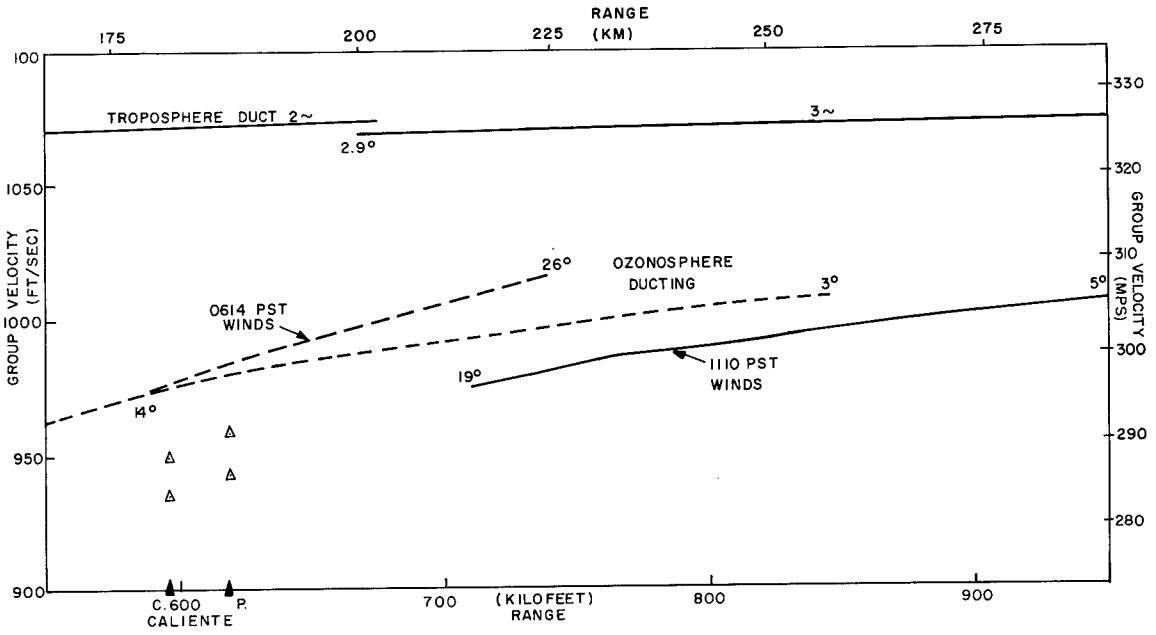

Figure 17. Calculated and observed group velocities, ENE, Caliente

A very weak signal duct was calculated for the surface 300-m layer, but this was no doubt blocked by the several intervening mountain ranges, for no early troposphere signal arrival could be found in the recordings.

Lund

Ray paths are shown in Figure 18 for light winds. This figure shows that the station was located in the main sound-ring from wind ducting at 40-km msl. Observed large pressure amplitudes and focus factors of nearly 4X were fairly well explained by this calculation (Figure 19). Observed group velocities were also in agreement with calculations (Figure 20).

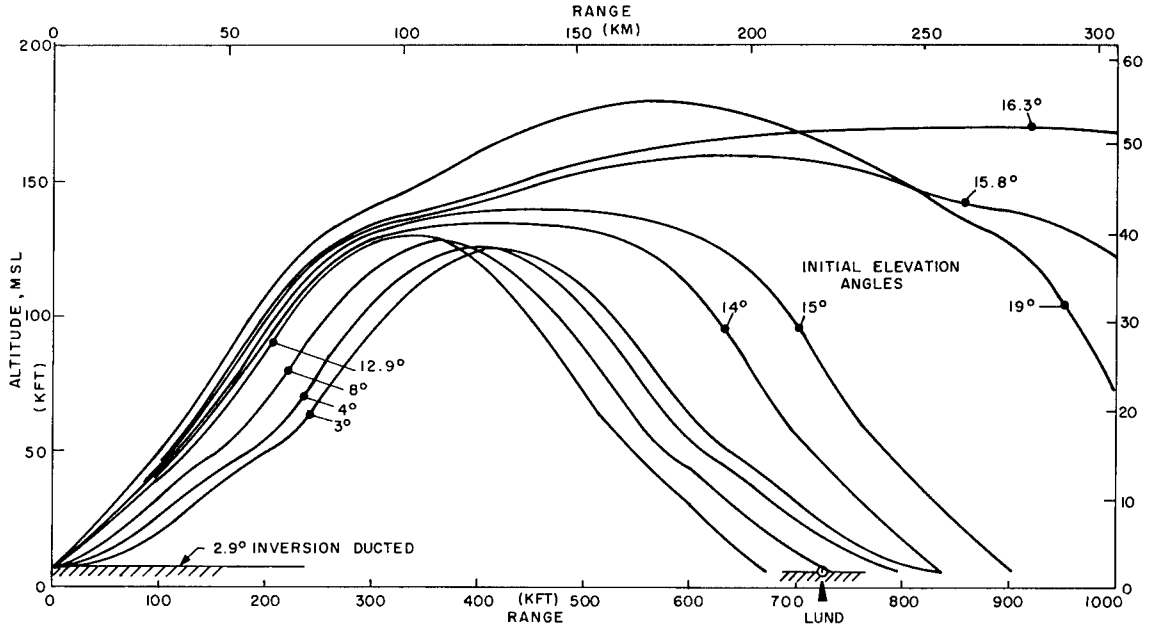

Figure 18. Ray paths, NNE direction, Lund

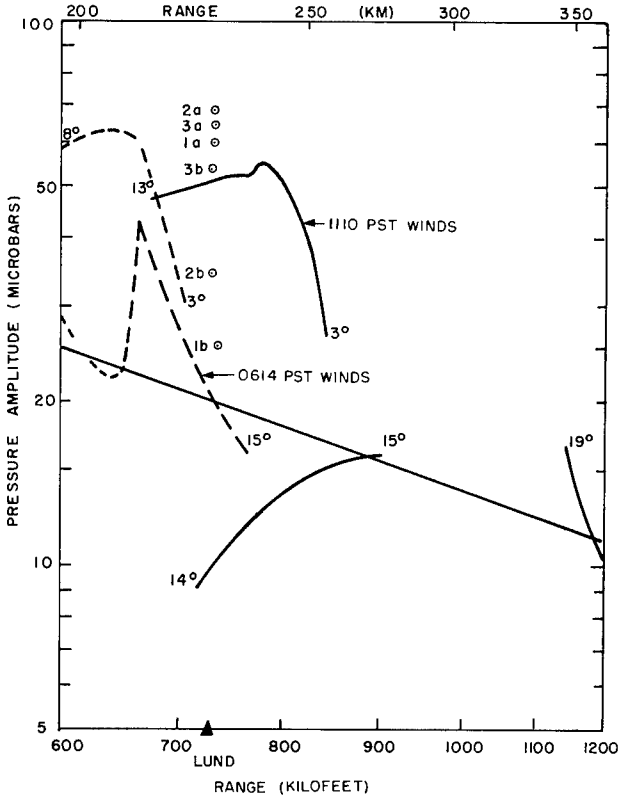

Figure 19.

Calculated and observed pressure amplitude, NNE direction, Lund

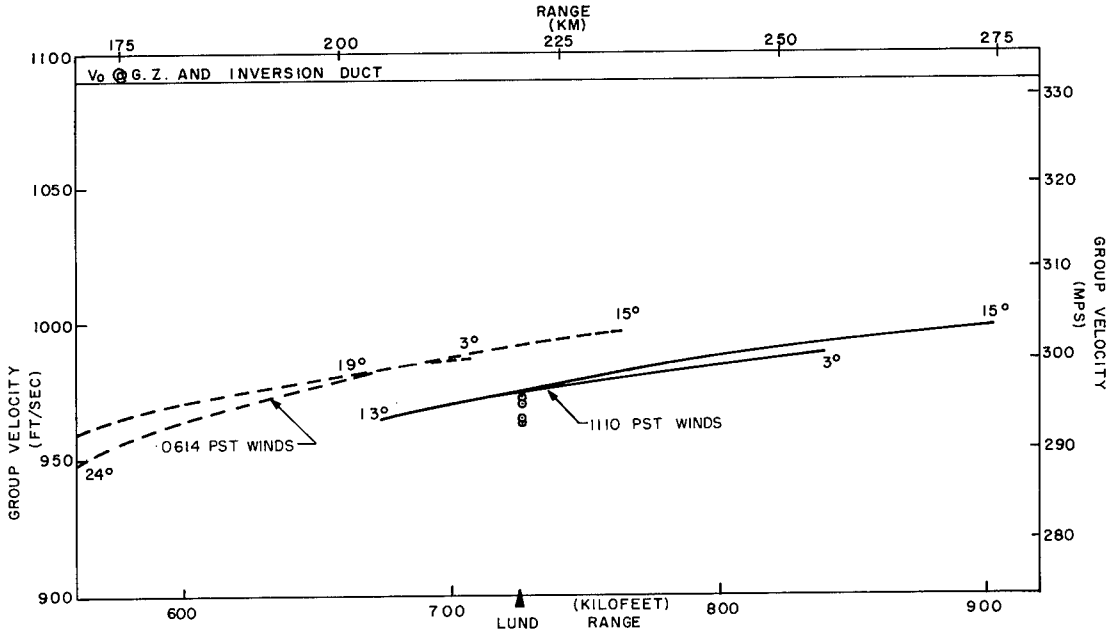

Figure 20. Calculated and observed group velocities, NNE direction, Lund

On the other hand, calculations from the high wind data showed that the main sound-ring landed far short of the Lund range, amplitudes were much lower in the outer fringes, and group velocities were 8 mps too fast.

No troposphere signal was detected to correlate with the 300-meter deep surface inversion duct shown by the calculation, but again, this duct was no doubt blocked by mountains.

In summary, the Lund data seem to tip the balance in favor of accepting the data obtained by the light wind speed rocket at 1110 PST. An adjustment to slightly higher winds at only one level, near 40-km msl, would serve to bring much better all around agreement with microbarograph data in the east and southeast directions, yet not hurt the agreement with propagations in other directions.

Summary

It is impossible, with the furnished rocket wind reports and single station microbarograph observations, to decide for certain whether ozonosphere wind speeds were generally light or strong. Accepting the lighter speeds, with minor adjustment and considering the accuracy of these chaff tracking measurements, seems to give the best fit for the amplitudes and arrival times of the collected microbarograph signals. If dual stations had been set up at one or two sites (two sensors about a mile apart on a line from the shot point), arrival incidence angles could have been computed for further signal path identification and verification checks.

Arrival times and group velocities at long ranges can usually be calculated within about 5 seconds and 2 mps, respectively. This seems very good in comparison with wind-speed measurement accuracy, but it does result from averaging out most random errors and variations over a thick layer of atmosphere.

Many observed amplitudes exceed calculated values, so there appears to be no overconservatism in focus factor determinations. On the other hand, where signals are consistently high, this cannot be attributed entirely to atmospheric turbulence effects. It would require a very careful, redundant set of experiments to establish whether the apparent average excursions were caused by wind field measurement errors or mistaken assumptions about standard propagation mechanisms.

There was no troposphere blast ducting toward Beatty or Goldfield, so they heard no rumbles and they were exposed to no airblast hazard. Because of the low yield and low transmissivity, there was no noticeable wave propagated into population centers east and southeast.

The mean transmissivity from Palanquin was $T = 0.026$; values were scattered with a logarithmic normal standard deviation of 0.451, so the $\pm 1\sigma$ range extended from $T = 0.017$ to $T = 0.041$. This scatter appears to be mostly attributable to amplitude variability between the calibration shots fired only a few minutes apart; the amplitude

variability was caused by atmospheric variability. This mean transmissivity is so low compared to results of other better-behaved cratering experiments that it must be ignored in extrapolation to other Plowshare activities.

References

1. Broyles, C. D., IBS Problem Curves, SCTM 268-56(51), Sandia Corporation, December 1, 1956 (OTS: $1.75).

2. Kelso, J. R., Stalk, G., and Clifford, C. C.; Project Banshee Field Operations, 1961 and 1962; Preliminary Report, DASA-543, Defense Atomic Support Agency, May 1963 (OUO).

3. Glasstone, S. (Ed.), The Effects of Nuclear Weapons, USDoD/USAEC, April 1962 (USGPO: $3.00).

4. Cox, E. F., Plagge, H. J., and Reed, J. W.; "Meteorology Directs Where Blast Will Strike," Bulletin of the American Meteorological Society, Vol. 35, No. 3, March 1954, pp. 95-103.

5. Cox, E. F., "Sound Propagation in Air," Handbuch der Physik, Vol. 48, Chapter 22, Springer-Verlag, Berlin (1958).

6. Cox, E. F., Plagge, H. J., and Reed, J. W.; Damaging Air Shocks at Large Distances from Explosions, Operation Buster-Jangle, WT-303, Sandia Corporation/AEC, April 24, 1952 (Unc).

7. Reed, J. W., Long-Distance Blast-Wave Attenuation by High-Explosives Charge Burial, SCTM 312-59(51), Sandia Corporation, September 21, 1959 (Unc).

8. Vortman, L. J., MacDougall, H. R., et al; Project Stagecoach, 20-Ton HE Cratering Experiment in Desert Alluvium, Final Report, SC-4595(RR), Sandia Corporation, May 1962 (OTS: $4.00).

9. Vortman, L. J., MacDougall, H. R., et al; Project Buckboard, 20-Ton and 1/2-Ton HE Cratering Experiments in Basalt Rock, Final Report, SC-4675(RR), Sandia Corp., August 1962 (OTS: $4.00).

10. Perret, W. R., Cahbai, A. J., Reed, J. W., and Vortman, L. J.; Project Scooter, Final Report, SC-4602(RR), Sandia Corporation, October 1963, (Unc).

11. Reed, J. W., and Church, H. W., Sedan Long Range Blast Propagation, Plowshare Project Sedan Final Report, PNE-202F, Sandia Corporation/AEC, August 30, 1963 (OTS: $.75).

12. Reed, J. W., Long-Range Air Blast Measurements and Interpretation, Project Danny Boy, POR-1809, Sandia Corporation/DoD/AEC, July 25, 1962 (CFRD).

13. Reed, J. W., Multiple Row Charge Blast Wave Observations at Long Range, Plowshare Project Dugout, PNE-607F, Sandia Corp/AEC, September 8, 1966, (FSTI: $1.50).

14. Friedman, M. P., Kane, D. J., and Sigalla, A.; "Effects of Atmosphere and Aircraft Motion on the Location and Intensity of a Sonic Boom," AIAA Journal, Vol. 1 (1963), pp. 1327-1335.

15. Maglieri, D. J., "Some Effects of Airplane Operations and the Atmosphere on Sonic Boom Signatures," J. Acoust. Soc. Amer. Vol. 39, No. 5, Part 2, May 1966, pp. S36-S42.

16. Reed, J. W., "Amplitude Variability of Explosion Waves at Long Ranges," J. Acoust. Soc. Amer. Vol. 39, No. 5, Part 1, May 1966, pp. 980-981.

17. Data Report, "Meteorological Rocket Network Firings," IRIG Document 10/9/62, Vol. XLIV, MWG, IRIG, RCC, White Sands Missile Range, New Mexico, February 1966.

18. U.S. Standard Atmosphere, 1962, NASA-USAF-USWB, USGPO, Washington, D.C., 1962.

19. Thompson, R. J., Sound Rays in the Atmosphere, SC-RR-64-1756, Sandia Corporation, January 1965 (Unc).

20. Thompson, R. J., Computing Sound Rays in the Presence of Wind, SC-RR-67-53, Sandia Corporation, February 1967 (Unc).

21. Maxim, J. A., Reed, J. W., and Shoemaker, F.; Microbarograph Operations Manual, SC-4942(M), Sandia Corporation, June 1964 (OUO).

22. Microbarograph Evaluation Report, SC-2990(TR), Division 5231, Sandia Corporation, September 18, 1953 (OTS: $1.50).

23. Bodhaine, B. A., Wind Attenuators for Microbarograph Measurements, SCTM-65-469, Sandia Corporation, October 1965 (Unc).

24. Vortman, L. J., and Shreve, J. D., Jr., The Effect of Height of Explosion on Blast Parameters, SC-3958(TR), Sandia Corporation, Albuquerque, New Mexico, June 20, 1956.

25. Church, H. W., Height-of-Burst Effects on Long-Range Propagated Blast Pressures, SC-4687(RR), Sandia Corp., May 1962 (Unc).

26. Reed, J. W., Air-Blast Yield Scaling in Refracting Atmospheres, SC-RR-65-369, Sandia Corporation, July 1965 (Unc).

27. Cox, E. F., and Reed, J. W., Long Distance Blast Predictions, Microbarograph Measurements, General Report on Weapons Tests, WT-9003, Sandia Corporation, September 1957 (SRD).

28. Vortman, L. J., Close-in Air Blast from a Cratering Nuclear Detonation in Rhyolite, Project Palanquin Report, PNE-902-F, Sandia Corp./AEC, April 1966 (CDI).

29. "Meteorological Equipment Data Accuracies," IRIG Document 110-64, Meteorological Working Group, Inter-Range Instrumentation Group, Range Commander Council, White Sands, Missile Range, New Mexico, March 1965.

PALANQUIN TECHNICAL REPORTS

Report No.	Agency	Author	Title
PNE-900F	LRL/EGG	R. Rohrer	Ground Motion and Cloud Photography
PNE-901F	LRL	C. Sisemore	Sub-Surface Effects
PNE-902F	SC	L. Vortman	Close-in Air Blast from a Cratering Nuclear Detonation in Rhyolite
PNE-903F	SC	J. Reed	Long-Range Air Blast
PNE-904F	NCG	F. Videon	Crater Topography
PNE-905F	NCG	P. Fisher	Pre-Shot Geological Engineering Properties
PNE-906F	LRL/N	L. Meyer	Geophysical Studies
PNE-907F	LRL	T. Gibson et al	Hazards Evaluation Measurements
PNE-908F	EG&G, Inc.	R. Rohrer	Scientific Photography
PNE-909F	LRL	J. Miskel N. Bonner et al	Radiochemical Studies
PNE-910F	USPHS	J. Coogan	Off-Site Surveillance
PNE-911F	REECo	B. Ubanks	On-Site Radiological Safety
PNE-912F	USWB		Weather and Radiation Support Activities
PNE-913F	R. F. Beers Inc.	L. Davis	Analysis of Surface Seismic Data

DISTRIBUTION LIST
(TID-4500, Category UC-35)

No. Copies	
1	AEC ALBUQUERQUE OPERATIONS OFFICE
1	AEC BETHESDA TECHNICAL LIBRARY
25	AEC DIVISION OF PEACEFUL NUCLEAR EXPLOSIVES
1	AEC LIBRARY, WASHINGTON
1	AEC MISSION TO THE IAEA
5	AEC NEVADA OPERATIONS OFFICE
1	AEC NEW YORK OPERATIONS OFFICE
1	AEC PATENT OFFICE
5	AEC SAN FRANCISCO OPERATIONS OFFICE
1	AEC SAVANNAH RIVER OPERATIONS OFFICE
1	AEC SCIENTIFIC REPRESENTATIVE, BELGIUM
1	AEC SCIENTIFIC REPRESENTATIVE, ENGLAND
1	AEROSPACE CORPORATION, SAN BERNARDINO (AF)
1	AIR FORCE AERO PROPULSION LABORATORY (APE)
1	AIR FORCE FOREIGN TECHNOLOGY DIVISION
1	AIR FORCE INSTITUTE OF TECHNOLOGY
1	AIR FORCE SCHOOL OF AEROSPACE MEDICINE
1	AIR FORCE WEAPONS LABORATORY
1	AMES LABORATORY (AEC)
1	ARGONNE NATIONAL LABORATORY (AEC)
8	ARMY ABERDEEN PROVING GROUND
1	ARMY CHIEF OF ENGINEERS
1	ARMY ELECTRONICS COMMAND
5	ARMY ENGINEER NUCLEAR CRATERING GROUP
6	ARMY ENGINEER WATERWAYS EXPERIMENT STATION
1	ARMY MATERIEL COMMAND
1	ARMY MEDICAL FIELD SERVICE SCHOOL
1	ARMY MEDICAL RESEARCH UNIT
1	ARMY MOBILITY EQUIPMENT RESEARCH AND DEVELOPMENT CENTER
1	ARMY OFFICE, CHIEF OF ENGINEERS
1	ARMY PICATINNY ARSENAL
1	ARMY ROCKY MOUNTAIN ARSENAL
1	ARMY SURGEON GENERAL
1	ARMY WALTER REED MEDICAL CENTER
1	ATOMIC POWER DEVELOPMENT ASSOCIATES, INC. (AEC)
2	ATOMICS INTERNATIONAL (AEC)
1	BABCOCK AND WILCOX COMPANY, ALLIANCE (AEC)
2	BATTELLE MEMORIAL INSTITUTE (AEC)
1	BATTELLE-NORTHWEST (AEC)
1	BROOKHAVEN NATIONAL LABORATORY (AEC)
2	BUREAU OF MINES, BARTLESVILLE (INT)
1	BUREAU OF MINES, DENVER (INT)
1	BUREAU OF MINES, LARAMIE (INT)
6	BUREAU OF RECLAMATION (INT)
1	DEPARTMENT OF AGRICULTURE NATIONAL LIBRARY
1	DOD DASA LIVERMORE
1	DOD DASA RADIOBIOLOGY RESEARCH INSTITUTE
1	DOD DASA SANDIA
1	DOD DASA WASHINGTON
1	DU PONT COMPANY, AIKEN (AEC)
1	DU PONT COMPANY, WILMINGTON (AEC)
1	EG&G, INC., ALBUQUERQUE (AEC)
1	EG&G, INC., LAS VEGAS (AEC)
5	EL PASO NATURAL GAS COMPANY (AEC)
8	ENVIRONMENTAL RESEARCH CORPORATION (AEC)
1	ENVIRONMENTAL RESEARCH CORPORATION, LAS VEGAS (AEC)
1	ENVIRONMENTAL SCIENCE SERVICES ADMINISTRATION, LAS VEGAS (COMM.)
1	ENVIRONMENTAL SCIENCE SERVICE ADMINISTRATION, MARYLAND (COMM.)
1	FRANKFORD ARSENAL (P-D LABS.)
1	GENERAL DYNAMICS/FORT WORTH (AF)

No. Copies	
1	GENERAL ELECTRIC COMPANY, CINCINNATI (AEC)
1	GENERAL ELECTRIC COMPANY, SAN JOSE (AEC)
1	GEOLOGICAL SURVEY, DENVER (INT)
1	GEOLOGICAL SURVEY, FLAGSTAFF (INT)
1	GEOLOGICAL SURVEY, MENLO PARK (INT)
1	GEOLOGICAL SURVEY (PECORA) (INT)
1	GULF GENERAL ATOMIC INCORPORATED (AEC)
2	HOLMES AND NARVER, INC. (AEC)
1	HUGHES AIRCRAFT COMPANY, FULLERTON (ARMY)
1	INSTITUTE FOR DEFENSE ANALYSIS (ARMY)
1	ISOTOPES, INC. (AEC)
1	JET PROPULSION LABORATORY (NASA)
1	JOHN A. BLUME AND ASSOCIATES (AEC)
1	LAWRENCE RADIATION LABORATORY, BERKELEY (AEC)
4	LAWRENCE RADIATION LABORATORY, LIVERMORE (AEC)
1	LIBRARY OF CONGRESS
2	LOS ALAMOS SCIENTIFIC LABORATORY (AEC)
5	LOVELACE FOUNDATION (AEC)
1	MASON AND HANGER-SILAS MASON CO., INC. AMARILLO (AEC)
1	MATHEMATICA (AEC)
1	MUESER, RUTLEDGE, WENTWORTH AND JOHNSTON (AEC)
1	MUTUAL ATOMIC ENERGY LIABILITY UNDERWRITERS (AEC)
1	NASA JOHN F. KENNEDY SPACE CENTER
1	NATIONAL BUREAU OF STANDARDS
1	NATIONAL INSTITUTES OF HEALTH (HEW)
1	NATIONAL REACTOR TESTING STATION (INC) (AEC)
1	NAVY ATOMIC ENERGY DIVISION
1	NAVY OFFICE OF NAVAL RESEARCH (CODE 422)
2	NAVY ORDNANCE LABORATORY
1	NAVY ORDNANCE SYSTEMS COMMAND
1	NAVY POSTGRADUATE SCHOOL
1	NAVY RADIOLOGICAL DEFENSE LABORATORY
1	NAVY SHIP SYSTEMS COMMAND HEADQUARTERS
1	NRA, INC. (DASA)
4	OAK RIDGE NATIONAL LABORATORY (AEC)
1	OHIO STATE UNIVERSITY (OCD)
1	PENNSYLVANIA STATE UNIVERSITY (AEC)
3	PUBLIC HEALTH SERVICE, LAS VEGAS (HEW)
1	PUBLIC HEALTH SERVICE, MONTGOMERY (HEW)
1	PUBLIC HEALTH SERVICE, ROCKVILLE (HEW)
1	PUBLIC HEALTH SERVICE, WINCHESTER (HEW)
1	PUERTO RICO NUCLEAR CENTER (AEC)
1	PURDUE UNIVERSITY (AEC)
1	RADIOPTICS, INC. (AEC)
2	REYNOLDS ELECTRICAL AND ENGINEERING COMPANY, INC. (AEC)
4	SANDIA CORPORATION, ALBUQUERQUE (AEC)
1	SANDIA CORPORATION, LIVERMORE (AEC)
1	SOUTHWEST RESEARCH INSTITUTE (AEC)
1	STANFORD UNIVERSITY (AEC)
1	UNION CARBIDE CORPORATION (ORGDP) (AEC)
1	UNIVERSITY OF CALIFORNIA, DAVIS, TALLEY (AEC)
1	UNIVERSITY OF CALIFORNIA, LOS ANGELES (AEC)
1	UNIVERSITY OF MICHIGAN (VESIAC) (ARMY)
1	UNIVERSITY OF ROCHESTER (KAPLON) (AEC)
1	UNIVERSITY OF TENNESSEE (AEC)
1	UNIVERSITY OF WASHINGTON (AEC)
1	WASHINGTON STATE UNIVERSITY (AEC)
1	WESTINGHOUSE ELECTRIC CORPORATION, (WAL) (AEC)
32	AEC DIVISION OF TECHNICAL INFORMATION EXTENSION
25	CLEARINGHOUSE FOR FEDERAL SCIENTIFIC AND TECHNICAL INFORMATION

PROJECT PALANQUIN

DISTRIBUTION LIST

1 D. J. Convey, Department of Mines and Technical Surveys, Ottawa, Ontario, Canada
1 Dr. G. W. Govier, Oil and Gas Conservation Board, Calgary, Alberta, Canada
1 U. S. Army Engineer Division, Lower Mississippi Valley, P. O. Box 80, Vicksburg, Mississippi 39181
1 U. S. Army Engineer District, 668 Federal Office Building, Memphis, Tennessee 38103
1 U. S. Army Engineer District, P. O. Box 60267, New Orleans, Louisiana 70160
1 U. S. Army Engineer District, 906 Olive Street, St. Louis, Missouri 63101
1 U. S. Army Engineer District, P. O. Box 60, Vicksburg, Mississippi 39181
1 U. S. Army Engineer Division, APO N. Y. 09019, Leghorn, Italy
1 U. S. Army Engineer District, GULF, APO N. Y. 09205, Teheran, Iran
1 U. S. Army Engineer Division, P. O. Box 103, Downtown Station, Omaha, Nebraska 68101
1 U. S. Army Engineer District, 1800 Federal Office Building, Kansas City, Missouri 64106
1 U. S. Army Engineer District, 6012 U. S. Post Office & Court House, 215 No. 17th Street, Omaha, Nebraska 68101
1 U. S. Army Engineer Division, 424 Trapelo Road, Waltham, Massachusetts 02154
1 U. S. Army Engineer Division, 90 Church Street, New York, New York 10007
1 U. S. Army Engineer District, P. O. Box 1715, Baltimore, Maryland 21203
1 U. S. Army Engineer District, 111 East 16th Street, New York, New York 10003
1 U. S. Army Engineer District, Ft. Norfolk, 803 Front Street, Norfolk, Virginia 23510
1 U. S. Army Engineer District, Custom House, 1nd & Chestnut Street, Philadelphia, Pennsylvania 19106
1 U. S. Army Engineer Division, 536 S. Clark Street, Chicago, Illinois 60605
1 U. S. Army Engineer District, Foot of Bridge Street, Buffalo, New York 14207
1 U. S. Army Engineer District, 219 S. Dearborn Street, Chicago, Illinois 60604
1 U. S. Army Engineer District, P. O. Box 1027, Detroit, Michigan 48231
1 U. S. Army Engineer District, Clock Tower Building, Rock Island, Illinois 61202
1 U. S. Army Engineer District, 1217 US PO & Customhouse, St. Paul, Minnesota 55101
1 U. S. Army Engineer District, Lake Survey, 630 Federal Building, Detroit, Michigan 48226
1 U. S. Army Engineer Division, 210 Custom House, Portland, Oregon 97209
1 U. S. Army Engineer District, 628 Pittock Block, Portland, Oregon 97205
1 U. S. Army Engineer District, P. O. Box 7002, Anchorage, Alaska 99051
1 U. S. Army Engineer District, 1519 Alaska Way, South, Seattle, Washington 98134
1 U. S. Army Engineer District, Building 602, City-County Airport, Walla Walla, Washington 99362
1 U. S. Army Engineer Division, P. O. Box 1159, Cincinnati, Ohio 45201
1 U. S. Army Engineer District, P. O. Box 2127, Huntington, West Virginia 25721
1 U. S. Army Engineer District, P. O. Box 59, Louisville, Kentucky 40201
1 U. S. Army Engineer District, P. O. Box 1070, Nashville, Tennessee 37202
1 U. S. Army Engineer District, 2032 Federal Building, 1000 Liberty Avenue, Pittsburg, Pennsylvania 15222
1 U. S. Army Engineer Division, Building 96, Fort Armstrong, Honolulu, Hawaii 96813
1 U. S. Army Engineer District, Far East, APO, San Francisco, California 96301
1 U. S. Army Engineer District, Building 96, Fort Armstrong, Honolulu, Hawaii 96813
1 U. S. Army Engineer District, Okinawa, APO, San Francisco, California 96331
1 U. S. Army Engineer Division, 510 Title Building, 30 Pryor Street SW., Atlanta, Georgia 30303
1 U. S. Army Engineer District, P. O. Box 1042, Merritt Island, Florida 32952
1 U. S. Army Engineer District, P. O. Box 905, Charleston, South Carolina 29402
1 U. S. Army Engineer District, P. O. Box 4970, Jacksonville, Florida 32201
1 U. S. Army Engineer District, P. O. Box 1169, Mobile, Alabama 36601
1 U. S. Army Engineer District, P. O. Box 889, Savannah, Georgia 31402
1 U. S. Army Engineer District, P. O. Box 1890, Wilmington, North Carolina 28402
1 U. S. Army Engineer Division, 630 Sansome Street, Room 1216, San Francisco, California 94111
1 U. S. Army Engineer District, P. O. Box 17277, Foy Station, Los Angeles, California 90017
1 U. S. Army Engineer District, 650 Capitol Mall, Sacramento, California 95814
1 U. S. Army Engineer District, 100 McAllister Street, San Francisco, California 94102
1 U. S. Army Engineer Division, 1114 Commerce Street, Dallas, Texas 75202
1 U. S. Army Engineer District, P. O. Box 1538, Albuquerque, New Mexico 87103
1 U. S. Army Engineer District, P. O. Box 1600, Fort Worth, Texas 76101
1 U. S. Army Engineer District, P. O. Box 1229, Galveston, Texas 77551
1 U. S. Army Engineer District, P. O. Box 867, Little Rock, Arkansas 72203
1 U. S. Army Engineer District, P. O. Box 61, Tulsa, Oklahoma 74102
1 U. S. Army Liaison Detachment, 111 E. 16th Street, New York, New York 10003
1 Mississippi River Commission, P. O. Box 80, Vicksburg, Mississippi 39181
1 Rivers and Harbors, Boards of Engineers, Temp C Building, 2nd & Q Streets SW., Washington, D. C. 20315
1 Corps of Engineer Ballistic Missile Construction Office, P. O. Box 4187, Norton Air Force Base, California 92409
1 U. S. Army Engineer Center, Ft. Belvoir, Virginia 22060
1 U. S. Army Engineer School, Ft. Belvoir, Virginia 22060
1 U. S. Army Engineering Reactors Group, Ft. Belvoir, Virginia 22060
1 U. S. Army Engineer Training Center, Ft. Leonard Wood, Missouri 65473
1 U. S. Coastal Engineering Research Board, 5201 Little Falls Road NW., Washington, D. C. 20016
75 U. S. Army Engineer Waterways Experiment Station, Vicksburg, Mississippi 39180
50 U. S. Army Engineer Nuclear Cratering Group, Livermore, California 94551